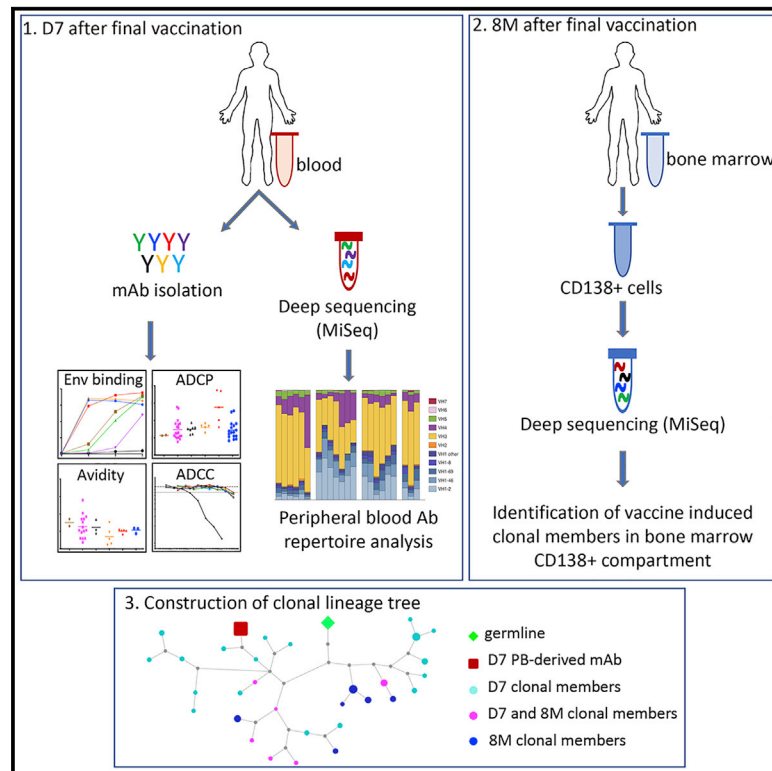


# Persistence of HIV-1 Env-Specific Plasmablast Lineages in Plasma Cells after Vaccination in Humans

## Graphical Abstract



## Authors

Madhubanti Basu,  
 Michael S. Piepenbrink,  
 Czestochowa Francois, ..., Jane Liesveld,  
 Michael C. Keefer, James J. Kobie

## Correspondence

jjkobie@uabmc.edu

## In Brief

In a phase I HIV vaccine trial, Basu et al. show the robust response of HIV Env gp120-specific peripheral blood plasmablasts immediately after vaccination, dominated by VH1 gene usage and V3 region-targeting Abs. They also define persistent linkage of these Env-reactive lineages to the bone marrow CD138<sup>+</sup> LLPC compartment.

## Highlights

- Assessed HIV Env-reactive peripheral blood plasmablast response post-vaccination
- Boosting with AIDSVAX B/E protein induced robust plasmablast responses
- Env-specific repertoire was dominated by VH1 gene usage and V3-region targeting Abs
- Plasmablast-derived lineages persisted in bone marrow CD138<sup>+</sup> long-lived plasma cells



## Article

# Persistence of HIV-1 Env-Specific Plasmablast Lineages in Plasma Cells after Vaccination in Humans

Madhubanti Basu,<sup>1</sup> Michael S. Piepenbrink,<sup>1</sup> Czesochowa Francois,<sup>2</sup> Fritzlaine Roche,<sup>2</sup> Bo Zheng,<sup>3</sup> David A. Spencer,<sup>4</sup> Ann J. Hessel,<sup>4</sup> Christopher F. Fucile,<sup>5</sup> Alexander F. Rosenberg,<sup>6</sup> Catherine A. Bunce,<sup>3</sup> Jane Liesveld,<sup>7</sup> Michael C. Keefer,<sup>3</sup> and James J. Kobie<sup>1,8,\*</sup>

<sup>1</sup>Infectious Diseases Division, University of Alabama at Birmingham, Birmingham, AL, USA

<sup>2</sup>School of Medicine, University of Rochester, Rochester, NY, USA

<sup>3</sup>Infectious Diseases Division, University of Rochester, Rochester, NY, USA

<sup>4</sup>Oregon National Primate Research Center, Oregon Health & Science University, Beaverton, OR, USA

<sup>5</sup>Informatics Institute, University of Alabama at Birmingham, Birmingham, AL, USA

<sup>6</sup>Department of Microbiology, University of Alabama at Birmingham, Birmingham, AL, USA

<sup>7</sup>Division of Hematology/Oncology, University of Rochester, Rochester, NY, USA

<sup>8</sup>Lead Contact

\*Correspondence: [jjkobie@uabmc.edu](mailto:jjkobie@uabmc.edu)

<https://doi.org/10.1016/j.xcrm.2020.100015>

## SUMMARY

Induction of persistent HIV-1 Envelope (Env) specific antibody (Ab) is a primary goal of HIV vaccine strategies; however, it is unclear whether HIV Env immunization in humans induces bone marrow plasma cells, the presumed source of long-lived systemic Ab. To define the features of Env-specific plasma cells after vaccination, samples were obtained from HVTN 105, a phase I trial testing the same gp120 protein immunogen, AIDSVAX B/E, used in RV144, along with a DNA immunogen in various prime and boost strategies. Boosting regimens that included AIDSVAX B/E induced robust peripheral blood plasmablast responses. The Env-specific immunoglobulin repertoire of the plasmablasts is dominated by VH1 gene usage and targeting of the V3 region. Numerous plasmablast-derived immunoglobulin lineages persisted in the bone marrow >8 months after immunization, including in the CD138<sup>+</sup> long-lived plasma cell compartment. These findings identify a cellular linkage for the development of sustained Env-specific Abs following vaccination in humans.

## INTRODUCTION

Despite increased access to antiretroviral therapies, HIV-1 is still a major health burden, with ~1.8 million new infections and ~900,000 HIV-related deaths globally in 2017.<sup>1</sup> Thus, the development of a safe and effective preventive HIV vaccine remains a global priority. Six HIV-1 vaccine efficacy trials have been completed so far and no vaccine has been licensed to date.<sup>2</sup> The RV144 trial, which included primarily low-risk participants and consisted of a canarypox virus vector (ALVAC) prime and a combination of clades B and E gp120 as a bivalent protein (AIDSVAX B/E) as a boost, is the only preventive HIV vaccine trial that has demonstrated protection thus far, although that protection is modest.<sup>3</sup> Protection against HIV-1 acquisition in RV144 was estimated at ~60% at 6 months and 31% at 42 months after final immunization.<sup>4</sup> Post hoc immune correlates studies indicated that efficacy was primarily correlated with the humoral response—more specifically, increased levels of HIV envelope (Env) V1V2 region-specific serum immunoglobulin G (IgG) in the presence of low Env-specific IgA correlated with a decreased risk of HIV-1 infection.<sup>5–8</sup> Follow-up studies showed that V1V2-

specific IgG3 responses correlated with decreased risk of HIV-1 infection; however, they rapidly disappeared from the serum, mirroring the waning efficacy observed over time in RV144.<sup>9,10</sup> IgG<sub>3</sub> has a short half-life, suggesting that a lack of sustained V1V2-specific IgG<sub>3</sub> production by long-lived plasma cells (LLPCs) was a critical barrier that reduced the clinical effectiveness of the RV144 regimen.

The potential protective activity of the antibodies (Abs) induced by RV144 has been suggested to be non-neutralizing and dependent on Fc receptor (FcR)-mediated effector functions, such as Ab-dependent cellular cytotoxicity (ADCC) and Ab-dependent cellular phagocytosis (ADCP).<sup>5,11,12</sup> In the presence of low Env-specific IgA, plasma ADCC activity correlated with a decreased risk of infection and appears to primarily target epitopes in V2 and C1. A substantial portion of the ADCC and ADCP activity induced by RV144 was mediated by IgG<sub>3</sub>,<sup>13</sup> and both ADCC and ADCP have been correlated with protection in several non-human primate challenge studies.<sup>10,14–16</sup> Thus, precise functional resolution of the AIDSVAX-induced B cell and Ab repertoire is likely consequential for a better understanding of HIV vaccine-mediated protection.



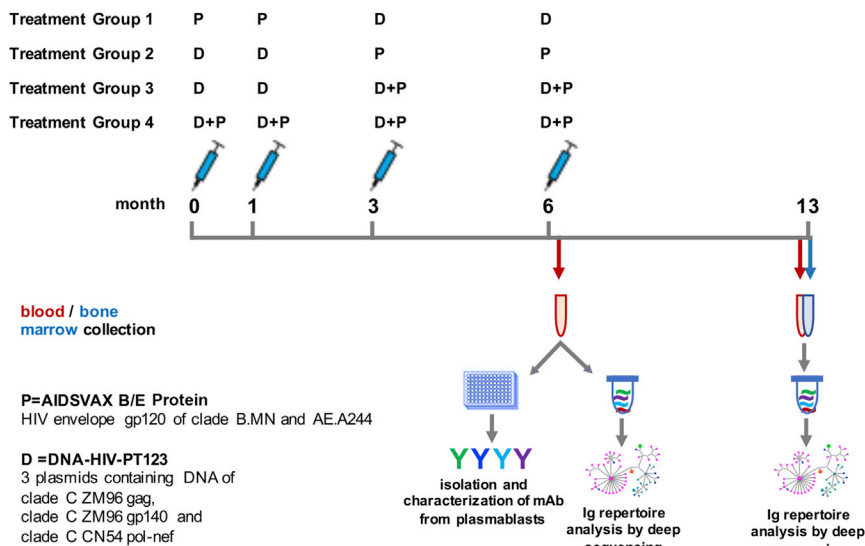


**Figure 1. Study Design**

Participants (n = 22) in HVTN 105 received AIDS-VAX B/E Protein (P) and DNA-HIV-PT123 plasmid (D) immunizations intramuscularly at months 0, 1, 3, and 6, according to the indicated schedule for each treatment group. Peripheral blood was collected at baseline (month 0) and 7 days (D7) after final immunization. Peripheral blood and bone marrow were collected 7–12 months after final immunization.

## RESULTS

### Boosting with AIDS-VAX B/E gp120 Protein Induces Peripheral Blood Plasmablasts

HVTN 105 participants received 4 vaccinations over a period of 6 months with different combinations of AIDS-VAX B/E bivalent gp120 protein, which includes

gp120 MN.B and gp120 A244.AE, and DNA-HIV-PT123, consisting of plasmids expressing 96ZM651.C gp140, ZM96.C gag, and CN54.C pol-nef (Figure 1). From a subset of participants, peripheral blood was obtained 7 days (D7) post-final vaccination. The majority (64%) of the participants had greater gp120 MN.B and A244.AE binding plasma IgG post-vaccination (Figures 2A and 2B). Overall, lower gp120 IgG was observed in the T1 group, which received booster vaccinations with DNA only. This is consistent with the findings of the overall plasma immunogenicity analysis of the trial that was previously reported.<sup>31</sup>

Acute infection or vaccination often triggers a rapid expansion of plasmablasts or antigen-specific Ab-secreting cells (ASCs), phenotypically defined as IgD<sup>-</sup>CD27<sup>hi</sup>CD38<sup>hi</sup>.<sup>17</sup> These plasmablasts peak in peripheral blood ~7 days after vaccination and then decline rapidly to nearly undetectable levels.<sup>18,19</sup> It is suggested that a subset of this population migrates to specialized niches in bone marrow (BM) and survives as LLPCs, typically defined as CD20<sup>-/low</sup> CD138<sup>+</sup>, and are thought to be the predominant source of long-lived serum Abs.<sup>20–22</sup> Other B cell populations, such as germinal center B cells, may also serve as the immediate precursors to LLPCs.<sup>23</sup> Long-lived circulating serum Abs derived from LLPCs provide sustained protection against viral infections such as mumps, measles, and influenza, but their persistence varies depending on the type of pathogens and vaccinations.<sup>24–27</sup> The findings of Montezuma-Rusca et al.<sup>28</sup> suggest that in HIV-1-infected individuals, circulating HIV-1-specific Abs are primarily derived from BM plasma cells. However, the observation by Huang et al.<sup>29</sup> that CD20<sup>+</sup> B cell depletion of an HIV-infected patient with rituximab, which does not act on LLPCs, resulted in a temporary ~2-fold decrease in serum neutralizing Ab and a reciprocal increase in HIV viremia, suggesting that circulating HIV Env-specific Abs during infection that contribute to viral suppression may be maintained in part by a short-lived CD20<sup>+</sup> Ab-secreting cell population. While the existence of HIV Env vaccine-induced LLPCs in BM has been shown in mice<sup>24</sup> and in non-human primates,<sup>30</sup> it has yet to be established in humans. Defining the mechanisms that regulate the induction of durable Ab-mediated protection in humans continues to be a key goal for effective HIV vaccine development.

Using samples obtained from HVTN 105, a phase I trial in which participants were immunized with the same bivalent gp120 protein, AIDS-VAX B/E, as used in RV144, combined with a clade C gp140-containing DNA immunogen in various prime/boost strategies,<sup>31</sup> we have assessed the response of HIV Env gp120 reactive plasmablasts in peripheral blood immediately after the final vaccination and defined their linkage to the CD138<sup>+</sup> long-lived bone marrow plasma cell compartment.

The presence of HIV gp120-specific IgG ASCs *ex vivo*, an indicator of peripheral blood plasmablasts, was observed D7 post-final vaccination as determined by ELISpot (Figures 2C and 2D). Overall, gp120-specific IgG ASCs were detected in 18 of 21 participants tested. Consistent with the plasma IgG response, the frequency of gp120-specific ASCs was lowest in the T1 group. Among T2–T4 groups, gp120<sup>+</sup> ASCs were 24% (range, 1%–77%) of the total IgG ASCs. These results indicate that immunizations with AIDS-VAX B/E induce a substantial gp120-specific IgG peripheral blood plasmablast response.

Consistent with the plasma IgG response, the frequency of gp120-specific ASCs was lowest in the T1 group. Among T2–T4 groups, gp120<sup>+</sup> ASCs were 24% (range, 1%–77%) of the total IgG ASCs. These results indicate that immunizations with AIDS-VAX B/E induce a substantial gp120-specific IgG peripheral blood plasmablast response.

### Peripheral Blood Plasmablasts Express gp120-Specific Monoclonal Abs (mAbs)

To define the fine specificity and molecular characteristics of the gp120-specific plasmablast response, plasmablasts (CD19<sup>+</sup>IgD<sup>-</sup>CD38<sup>+</sup>CD27<sup>2+</sup>) were single-cell sorted (Figure 3A) from the peripheral blood D7 post-final vaccination. The plasmablasts were predominantly CD20<sup>-</sup>CD126(IL-6R $\alpha$ )<sup>+</sup>, consistent with an antigen-specific response.<sup>32</sup> Following cDNA synthesis, PCR amplification, and transient expression of Igs, gp120-reactive mAbs (156 total from 10 participants) were identified by screening ELISA and cloned into full IgG<sub>1</sub> expression vectors. Cloned mAbs were tested for their binding activity and only mAbs having OD<sub>450</sub>  $\geq$  1 at 10  $\mu$ g/mL against at least one HIV gp120 from the vaccine component strains (MN.B [AIDS-VAX B/E], A244.AE [AIDS-VAX B/E], and 96ZM651.C [PT123 DNA]) were further studied (Figure 3B). These resulting 66 mAbs from

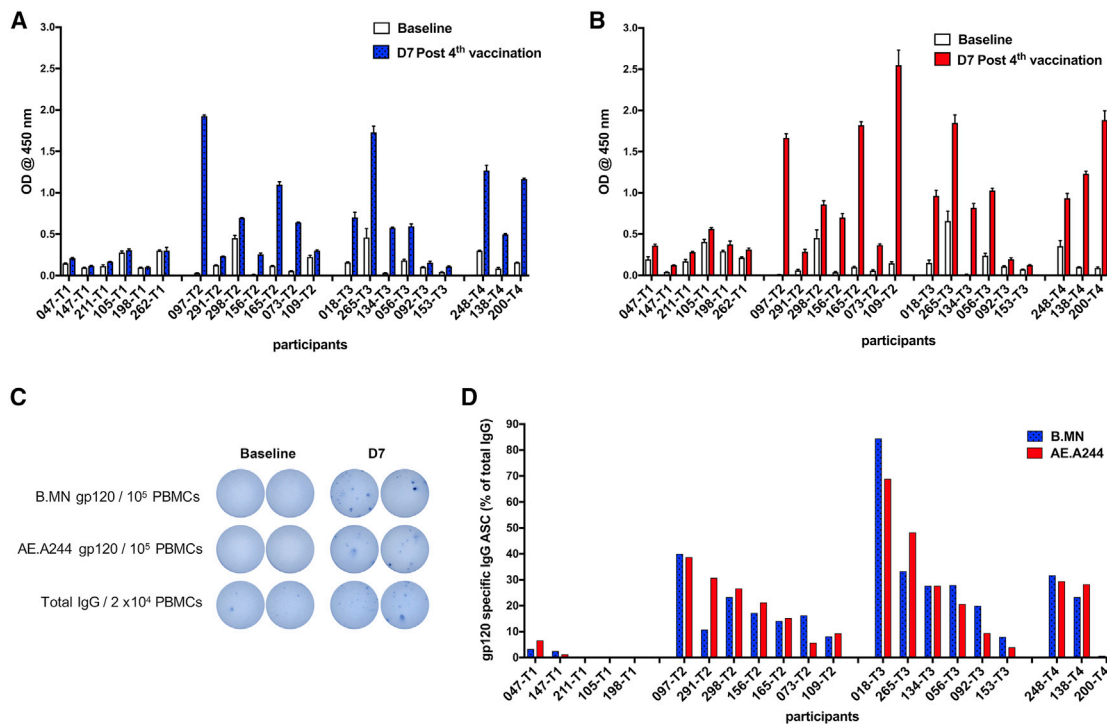


**Figure 2. Boosting with AIDSVAx B/E gp120 Protein Induces Peripheral Blood Plasmablasts**

(A and B) Plasma ( $n = 22$ ) collected at baseline and D7 following the final immunization was tested by ELISA ( $n = 3$  replicates per dilution) for IgG specific to gp120 MN.B (A) and gp120 A244.AE (B) at 1:2500 dilution. Each bar represents mean  $\pm$  SEM for an individual participant. Participant number and treatment group (T) indicated. The frequency of total IgG and gp120-specific IgG-secreting cells was determined by Elispot ( $n = 3$  replicates per dilution).

(C) Representative Elispot results from a single participant.

(D) Frequency of gp120<sup>+</sup> IgG antibody (Ab)-secreting cells (ASC) at D7 after final immunization. Bars indicate frequency for an individual participant based on triplicate Elispot wells.

8 participants were defined as gp120<sup>+</sup> and evaluated further. Nearly half (47%) of these plasmablast-derived gp120<sup>+</sup> mAbs are reactive against all 3 gp120s present in the vaccine (Figure 3C). Nearly all of the mAbs (94%) displayed MN.B reactivity, among which 50% were also reactive to A244.AE and 96ZM651.C, while 37% of the MN.B reactive mAbs were exclusive to MN.B. Very few mAbs (4.5%) were reactive to AE.A244 exclusively, and none were reactive to C.96ZM651 exclusively. Due to the limited number of participants per group for this sub-study, comparisons of the mAbs between groups was not pursued.

To determine the gross epitope specificity of isolated mAbs, the mAbs were tested by ELISA using overlapping linear peptides spanning the gp160 Env (MN.B or M.Cons strains) or Env region-specific antigens, including V1V2 scaffolds, V3 peptides, and CD4-binding site emphasizing Resurfaced Core 3 (RSC3) proteins. We could successfully map 10/66 (15%) mAbs against specific regions of the Env (Figure 3D; Table S1); of those, 5 were specific for the V3 loop, with 2 each recognizing C1 and V1V2, and a single mAb recognizing C5. No CD4 binding site-specific Abs were evident among the mAbs. Four of the five V3-specific mAbs bind to the V3 crown area, with a putative epitope contained within the NYNKRKRIHIG linear sequence, and use either VH5-51 or VH1-24 along with V $\lambda$ , which has previously been shown to be common among V3-specific mAbs.<sup>33,34</sup> As the

binding of only  $\sim$ 12% of MN.B- or M.Cons-specific mAbs could be mapped to linear peptides, it suggests that the majority of the mAbs recognize conformational epitopes. These results suggest that the gp120-specific plasmablast response is dominated by mAbs with cross-clade binding activity, for which recognition of conformational epitopes is dominant and V1V2 and CD4bs specificity is subdominant.

### Plasmablast-Derived mAbs Include Those with High Avidity and ADCP Functionality

To ascertain the avidity of the mAbs for gp120, their binding stability was determined in the presence of the chaotropic agent 8M urea. Most of the mAbs (51/66) retained at least 80% of their binding activity (avidity index of  $\geq 0.8$ ) to at least one of the vaccine's gp120s, and the majority (35/66) retained all of their binding activity (Figure 4A). The ability of the mAbs to mediate ADCP, a Fc-mediated effector function, was determined using HIV-1 Env MN.B and A244.AE gp120-coated beads. Approximately half (34/66) of the mAbs could mediate at least modest ADCP (ADCP score  $\geq 1.25$ ), with a subset of mAbs (11/66) that had substantial ADCP activity (ADCP score  $\geq 2.0$ ) (Figure 4B). Overall, a trend toward greater ADCP activity against A244.AE was observed compared to MN.B. No association between epitope specificity, avidity, or ADCP activity was apparent. Although many of the mAbs exhibited high binding activity and ability to

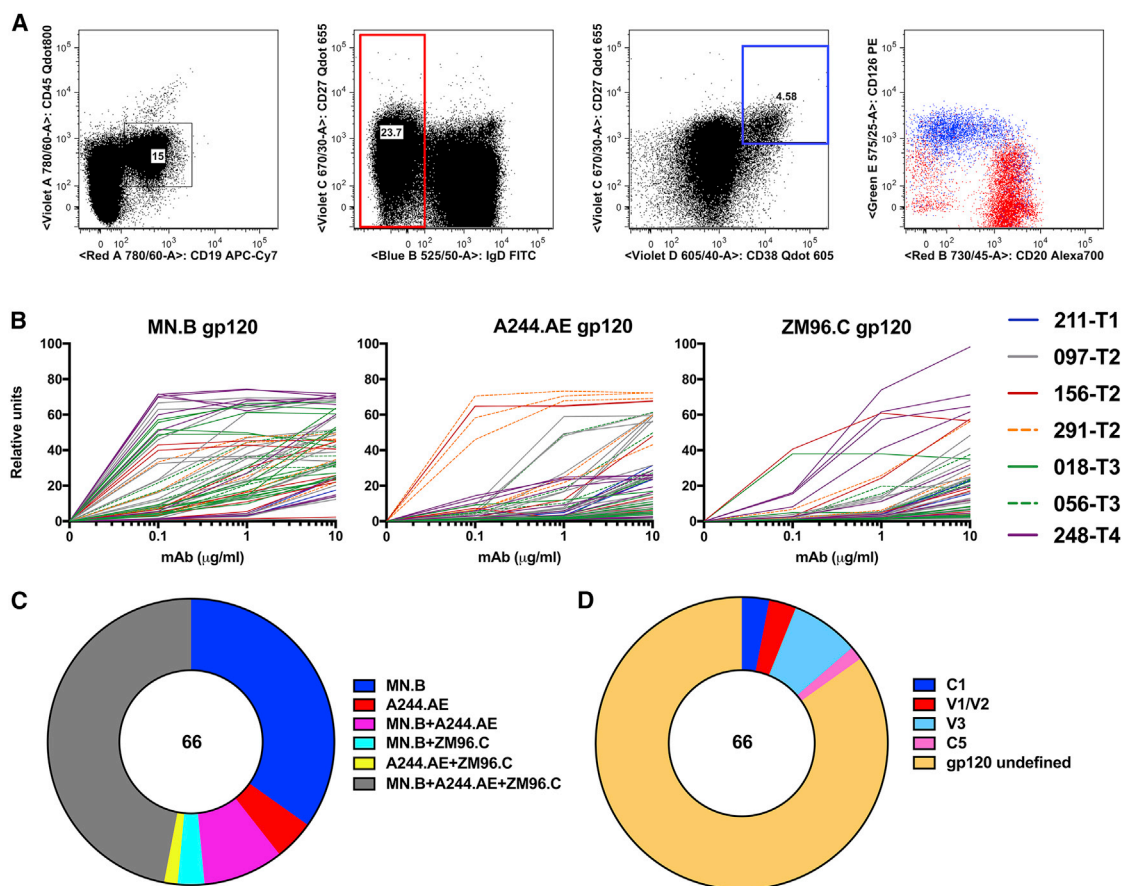


**Figure 3. Peripheral Blood Plasmablasts Express gp120-Specific Monoclonal Antibodies (mAbs)**

(A) Gating strategy to isolate peripheral blood plasmablasts (IgD-CD38<sup>+</sup>CD27<sup>+</sup>) D7 after final immunization.

(B) Reactivity of mAbs (n = 66) to gp120 determined by ELISA (n = 3 replicates per dilution). Each line represents the mean of an individual mAb.

(C) Summary of gp120 binding profiles of mAbs.

(D) Summary of gp120 region-specific binding profiles of mAbs.

mediate ADCC, most of the mAbs did not exhibit ADCC against infected cells, with only 6 mAbs having weak ADCC activity (~20%–35% reduction at 50  $\mu\text{g}/\text{mL}$ ) (Figure 4C). Most of the mAbs did not exhibit neutralizing activity; however, 6 mAbs were able to neutralize tier 1 SF162 virus (Figure 4D).

### VH-1 Usage Dominates the HIV-Env-Specific Plasmablast Repertoire

The variable regions of the heavy- and light-chain genes of the mAbs were sequenced to determine their Ig gene usage and characteristics (Figure 5; Table S1). VH1 family usage predominated and was used by 61% of the mAbs, with VH1-2 (39%) and VH1-46 (12%) gene usage most highly represented among the isolated mAbs (Figure 5A) and is consistent with previously published results.<sup>12</sup> We critically analyzed the sequences of the VH1-2\*02 Abs 7/66 (~11%) for VRC01 class Ab features,<sup>35,36</sup> but found that none of them were VRC01 class Ab (not shown); most notably, Trp100B is absent in the heavy chain, and the light-chain complementarity determining region 3 (LCDR3) length was consistently >8 amino acids. This is also consistent

with none of the mAbs appearing to be CD4 binding site specific and with the lack of induction of tier 2 plasma-neutralizing Abs.<sup>31</sup>

A trait of some broadly neutralizing Abs (bNAbs) against HIV-1 is the presence of high numbers of somatic mutations. Overall, the average amino acid VH mutation from germline was 6.9% (3.7% nt) (Figure 5B; Table S1). This is higher than the mutation frequency for AIDSVAX B/E-elicited mAbs, as previously reported (2.4% nt),<sup>12</sup> but somewhat lower than the Abs isolated from RV305 (6.99% nt), a follow-up trial on RV144 participants that remained HIV uninfected and received a booster with the same immunogens, including AIDSVAX B/E 6 to 8 years after the completion of RV144.<sup>37</sup> The heavy-chain complementarity determining region 3s (HCDR3s) of most of the mAbs were 8–21 amino acids, with an average of 14 amino acids long; however, 10/66 (15%) mAbs had HCDR3s of  $\geq 22$  amino acids in length (Figure 5C), a common feature of many HIV-1 bNAbs.<sup>38–42</sup>

Sequence analysis of the constant region 1 (CH1) domain of the native mAbs revealed that, as expected, most mAbs were IgGs (Figure 5D). IgG<sub>1</sub> was overwhelmingly dominant (79%), with a limited representation of IgG<sub>3</sub> (5%) and single IgG<sub>2</sub> mAbs (2%). IgA<sub>1</sub> made up 9% of the mAbs, along with a single

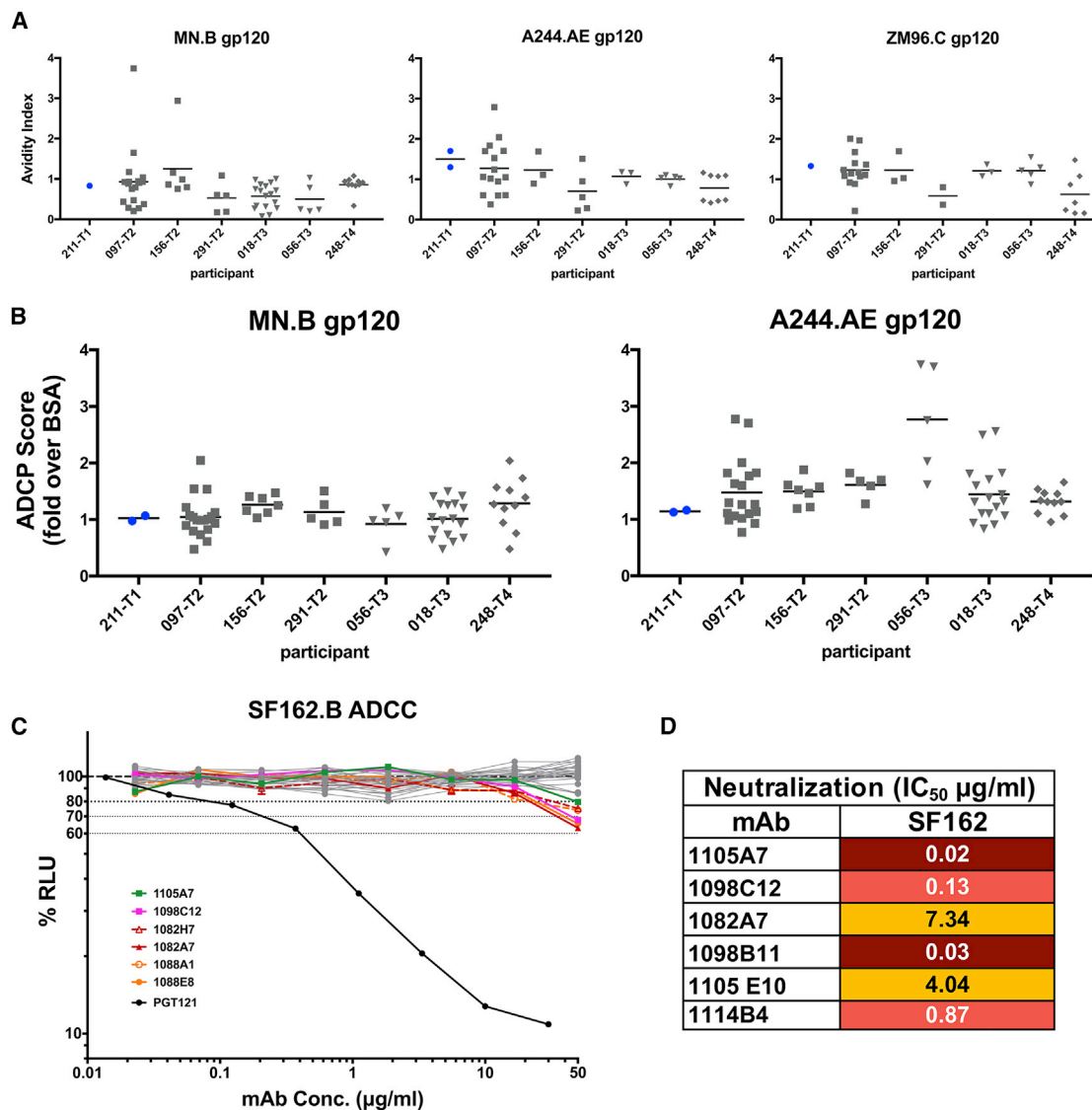


**Figure 4. Plasmablast-Derived mAbs Include Those with High Avidity and ADCC Functionality**

(A) The avidity of the mAbs binding to gp120 in the presence of 8M urea was determined by ELISA (n = 3 replicates). Each symbol represents the avidity index for an individual mAb as determined from triplicates.  
 (B) The Ab-dependent cellular phagocytosis of gp120-coated and BSA-coated fluorescent beads was determined at 5 µg/mL mAb. Each symbol represents the ADCP score for an individual mAb. Blue symbols denote T1 participant.  
 (C) mAbs were serially diluted starting at 50 µg/mL and tested in duplicate for ADCC against SHIV-SF162P3.B-infected NKR24 reporter cells.  
 (D) mAbs were serially diluted and tested in duplicate at each dilution for neutralizing activity against SF162.B pseudoviruses in the standardized TZM-bl assay.

IgA<sub>2</sub> mAb (2%). The IgA mAbs were predominantly non-VH1 (only 29% VH1) and trended toward greater somatic hypermutation (13.1%) (Table S1). IgM made up 5% of the mAbs.

To obtain a more comprehensive perspective on the HIV-1 Env vaccine-induced B cell repertoire, VH deep sequencing of the expressed IgG of peripheral blood B cells was done at D7, the same time point from which the mAbs were isolated. It is anticipated that at this time point, the expressed IgG repertoire is dominated by plasmablasts. The usage of VH1 was elevated in T2, T3, and T4 participants, making up over 40% of the clonal lineages from the majority of the T2 and T3 participants (Figure 6A).

VH1-2 dominated the largest lineages in most T2–T4 participants (Figure 6B), and was used by 26.1%, 16.0%, and 8.1% of the lineages in the T2, T3, and T4 participants, respectively, compared to only 3.7% in the T1 participants. The VH1-46 usage was similarly increased, although to a lesser extent, comprising 13.3%, 10.2%, and 5.6% of the lineages in T2, T3, and T4 participants, respectively, and only 2.6% in the T1 participants (Figure 6A). The increases in VH1-2 and VH1-46 usage compared to T1 were significant for T2 (p = 0.0012, 0.0012) and T3 (p = 0.0087, 0.0022). The expansion of VH1 lineages among T2, T3, and T4 participants is consistent with the VH1 bias observed in the

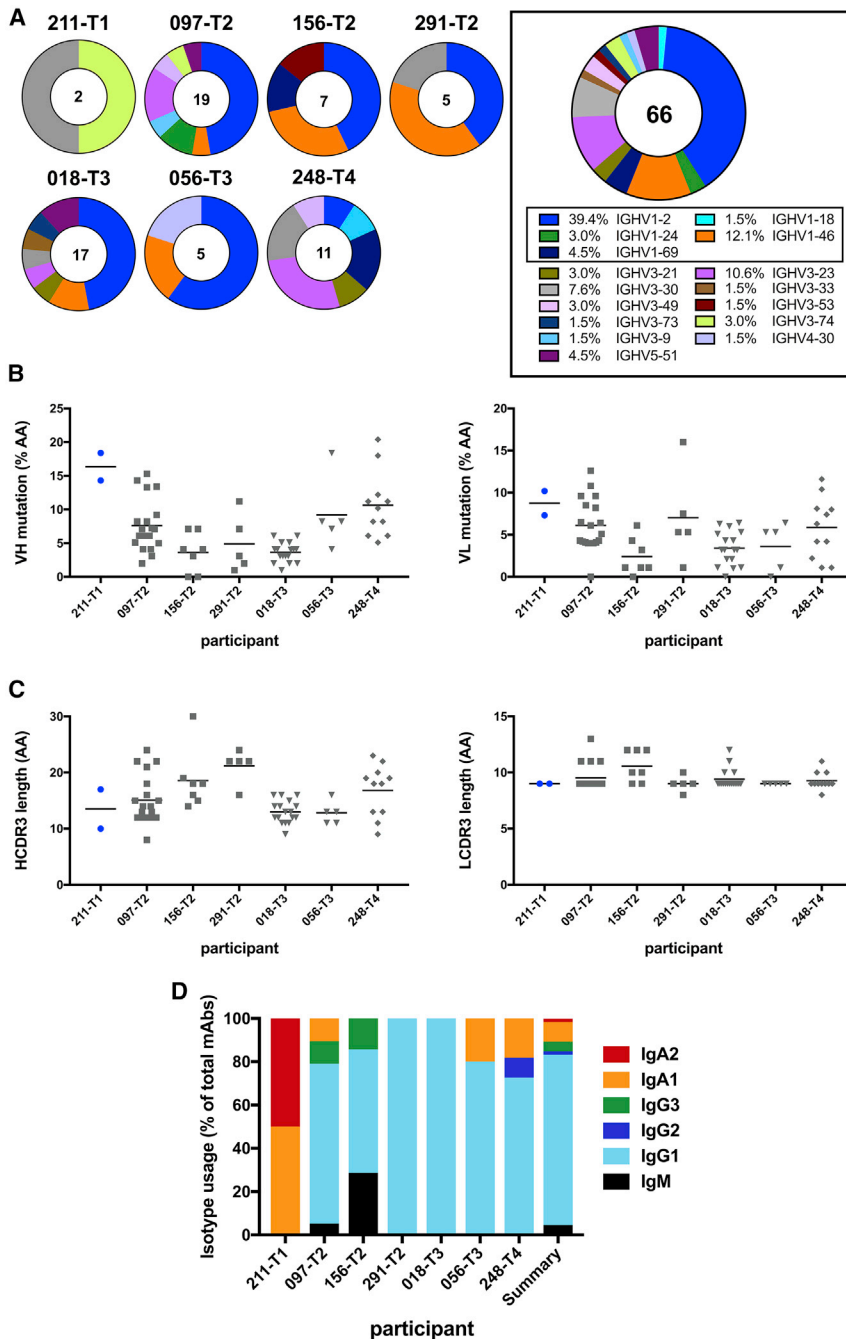


**Figure 5. Molecular Characteristics of Plasmablast-Derived mAbs**

(A) VH gene usage of mAbs isolated from indicated individual and in summary.

(B) Mutation from germline for VH and VL for individual mAbs presented.

(C) Length of CDR3 for heavy and light chain indicated. Blue symbols denote T1 participant.

(D) Distribution of isotype usage of mAbs among each individual and in summary.

higher frequency of long HCDR3s (19.0% versus 11.0%), as defined as  $\geq 22$  amino acids (Figure 6D). The T2–T4 VH1-2 lineages are moderately mutated from germline (3.1% nt) (Figure 6E). The VH1-2 sequences in the T2–T4 participants are dominated by IgG<sub>1</sub> usage, with minor usage of other IgG subclasses, including modestly increased IgG<sub>4</sub> usage evident among T4 participants (Figure 6F), which is consistent with plasma Env-specific Abs reported previously in this group.<sup>31</sup> Among the VH1-2 sequences in the T2–T4 participants, the IgG<sub>4</sub> and IgG<sub>2</sub> sequences exhibited the greatest somatic hypermutation (4.1% and 3.7%, respectively) compared to IgG<sub>1</sub> and IgG<sub>3</sub> sequences (3.1% and 2.7%, respectively) (Figure 6G), which is consistent with their germline exon order and IgG<sub>4</sub> developing as a result of repeated antigen exposure.<sup>43</sup>

### Persistence of HIV Env-Specific Plasmablast Lineages in the BM LLPC

Long-lived bone marrow resident plasma cells are the presumed source of sustained circulating plasma Abs and also a contributor to IgG at mucosal sites due to transudation.<sup>44–46</sup> We sought to determine whether immunization with HIV-1 Env induces LLPCs in humans. BM obtained 8–12 months after the final immunization was assessed by EliSpot for Env-specific ASCs. Despite detecting ASCs specific for influenza in the BM, including within

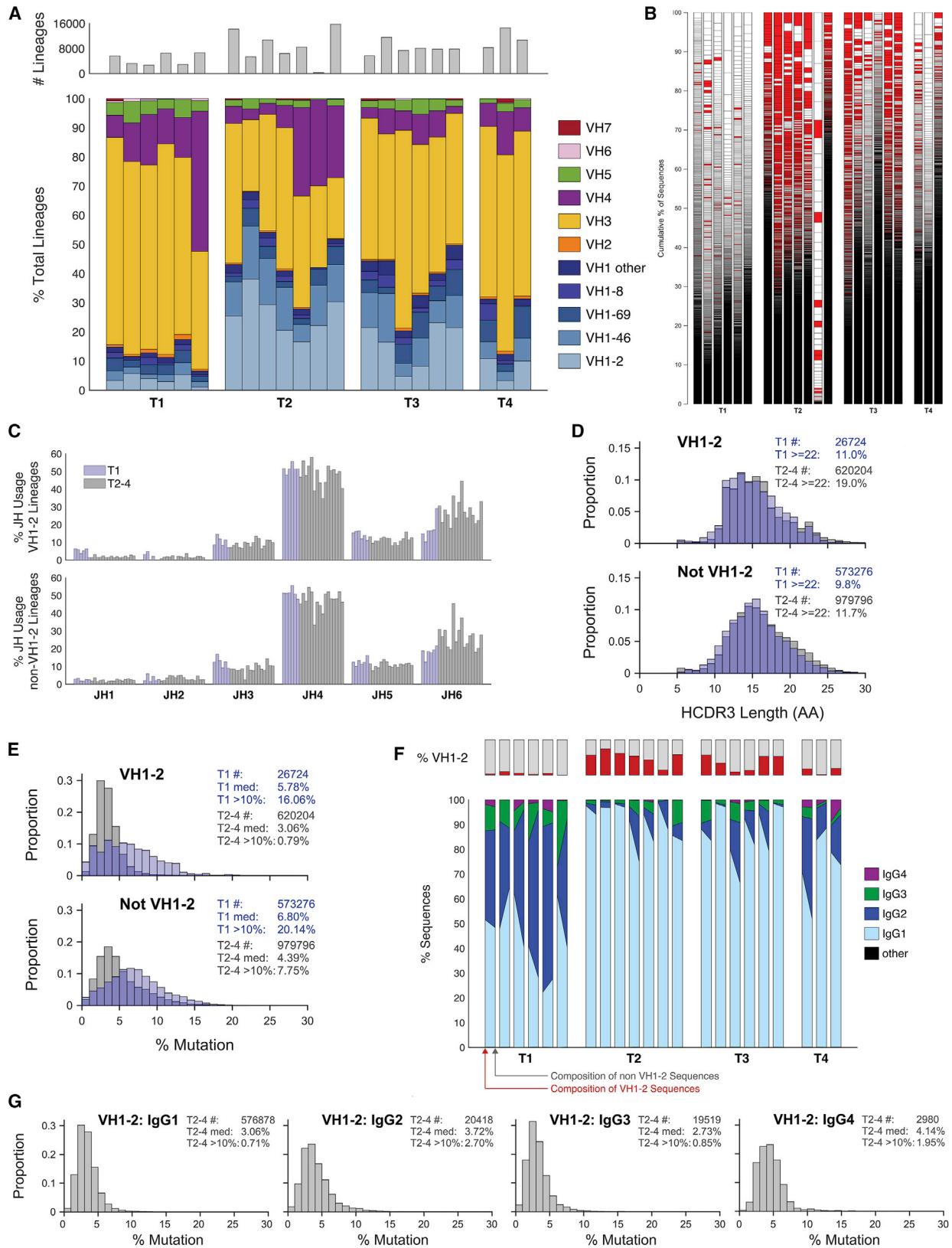
the CD138<sup>+</sup> LLPC compartment, HIV-1 Env-specific ASCs were not reliably detected within the BM by EliSpot (Figure 7A), suggesting that they are not present at sufficient quantities above the level of detection for the EliSpot. Therefore, we performed VH deep sequencing to determine whether members of the clonal lineages represented by the Env-specific mAbs isolated from D7 peripheral blood plasmablasts were present in the BM. Of the 52 mAbs isolated from 4 participants from which BM had been obtained, members of 19 of these mAb clonal lineages were present in the BM, 9 of which were found among CD138<sup>+</sup> LLPCs (Figure 7B). No obvious

mAbs obtained (Figure 5A), and the minimal HIV-1 Env-specific plasma Ab and plasmablast response observed at this time point in T1 (Figure 2) suggests that the VH1 expansion among the IgG repertoire in those participants not in T1 (i.e., T2, T3, and T4) is a consequence of the most recent AIDS VAX B/E immunization.

Focusing on the VH1-2 lineages in the T2, T3, and T4 participants, as they represent the HIV-1 Env-specific IgG repertoire, we observe that compared to T1, they exhibit a significant bias toward decreased heavy chain J1 gene (JH1) ( $p = 0.0110$ ) and increased JH6 ( $p = 0.0057$ ) usage (Figure 6C) and corresponding

mAbs obtained (Figure 5A), and the minimal HIV-1 Env-specific plasma Ab and plasmablast response observed at this time point in T1 (Figure 2) suggests that the VH1 expansion among the IgG repertoire in those participants not in T1 (i.e., T2, T3, and T4) is a consequence of the most recent AIDS VAX B/E immunization.

Focusing on the VH1-2 lineages in the T2, T3, and T4 participants, as they represent the HIV-1 Env-specific IgG repertoire, we observe that compared to T1, they exhibit a significant bias toward decreased heavy chain J1 gene (JH1) ( $p = 0.0110$ ) and increased JH6 ( $p = 0.0057$ ) usage (Figure 6C) and corresponding



(legend on next page)



distinct binding, functional, or molecular features distinguished the mAbs for which clonal lineage members were found in BM compared to those that were not (Figure S1).

The 1105E9 mAb lineage, isolated from 018-T3, uses VH1-2\*06 and included numerous clonal members among BM CD138<sup>+</sup> LLPCs (Figure 7C). The 1105E9 and the CD138<sup>+</sup> LLPC lineage members share the M37I mutation from germline in FR2, G56D mutation in CDR2, and N58Y mutation in FR3. The 1105E9 lineage was dominated by IgG<sub>1</sub> usage.

The mAbs 1098D3 and 1098F3 belong to the same lineage that uses VH1-2\*06. This lineage was isolated from 097-T2 and includes clonal members among CD138<sup>+</sup> LLPCs (Figure 7D). Both 1098D3 and 1098F3, along with the CD138<sup>+</sup> LLPC lineage members, share T33I mutation from germline in CDR1. The lineage is dominated by IgG<sub>1</sub> usage, and includes minor instances of IgG<sub>2</sub>, IgG<sub>3</sub>, and IgG<sub>4</sub> usage. The LLPC lineage members appear to segregate on a continuum of degree of somatic hypermutation, including those less mutated and further mutated than the 1098D3 and 1098F3 mAbs. Lineage members were also present in the peripheral blood 8 months (M8) after immunization, indicating this lineage is also persisting among peripheral memory B cells.

The mAbs 1098B8 and 1098C4 belong to the same lineage, were also isolated from 097-T2, are C1 specific, and use VH1-2\*06, and the lineage includes CD138<sup>+</sup> LLPCs (Figure 7E). The lineage is dominated by IgG<sub>1</sub> usage, but includes instances of IgG<sub>2</sub>, IgG<sub>3</sub>, IgG<sub>4</sub>, and IgA usage. 1098B8, which is less mutated from germline (GL) compared to 1098C4, was isolated as an IgG<sub>1</sub> and similarly its nearest neighbors are dominated by IgG<sub>1</sub>. 1098C4, an IgG<sub>3</sub>, and its nearest neighbors are similarly dominated by IgG<sub>3</sub> usage. Both 1098B8 and 1098C4, along with the CD138<sup>+</sup> LLPC lineage members, are mutated at G56 in CDR2. In addition, lineage members persist in the peripheral blood memory B cells 8 months after immunization, including a cluster that is proximal to the 1098C4 mAb cluster, and a cluster that is quite distal from the 1098C4 and 1098B8 clusters.

These results indicate that HIV-1 Env-specific LLPCs are generated in humans following HIV Env immunization. These HIV-1 Env-specific LLPCs include a population that is clonally related to D7 peripheral blood plasmablasts and persistent peripheral blood memory B cells.

## DISCUSSION

Plasmablasts offer a window into the early dynamics of the HIV-1 vaccine-induced humoral response. The HVTN 105 vaccine

regimen, particularly boosting with AIDSVAX B/E Env protein, resulted in the robust induction of Env-specific plasmablasts, with the majority capable of recognizing Env from multiple clades. There was dominant usage of VH1-2 among the Env-specific plasmablast repertoire, and numerous instances of the persistence of clonal lineage members among BM LLPCs, demonstrating the linkage of these populations, which may have implications for regulating the durability of Ab responses to HIV Env.

Although the mAbs described here are the first reported to be derived from HIV vaccine-induced human plasmablasts, mAbs have been isolated from human peripheral blood memory B cells following HIV vaccination, including from AIDSVAX vaccine recipients. A significant portion of AIDSVAX-induced memory B cell-derived mAbs were directed against the first constant region (C1) of gp120 Env protein.<sup>12</sup> In addition, 2 mAbs, CH58 and CH59, were identified to have specific affinity for position K169 on the gp120 V2 region and partially overlap the binding region of the broadly neutralizing mAbs CH01 and PG9.<sup>47</sup> Only a minority of the mAbs we isolated were specific for C1 or V1/V2; however, 5 V3-specific mAbs were isolated. The V3-specific mAbs primarily recognized the V3 crown epitope NYNKRKRIHIG, and based on their reactivity profile and for 2 of the mAbs (1105A7 and 1114B4), their VH5-51 usage, it is likely they are binding the V3 crown in the cradle mode,<sup>34</sup> which is the predominant type of V3 mAbs induced by vaccination, including in AIDSVAX trials; VAX003 and VAX004.<sup>33,48–50</sup> Although AIDSVAX has induced only modest tier 1 neutralizing plasma Abs, the majority of Abs in RV144 were targeted to V3, and V3 Abs inversely correlated with the risk of infection in RV144.<sup>51</sup> In addition, RV144 resulted in Ab-mediated immune pressure on V3 among infecting viruses.<sup>52</sup> Overall, only a few of the plasmablast-derived mAbs we isolated exhibited neutralizing activity; several notably were V3 specific, including 1098C12, 1105A7, 1098B11, and 1114B4. Our characterization of the potential epitopes recognized by the plasmablast-isolated mAbs was very limited and should be expanded upon, particularly for those mAbs with substantial functional activity. Further resolution of the precise epitope specificity of these AIDSVAX plasmablast-derived mAbs, including V3 binding mode, may provide further insight into the protection induced in RV144.

Although a few CD4bs-specific mAbs with sporadic tier 1 and tier 2 neutralizing activity were isolated from RV305,<sup>37</sup> CD4bs specificity was not evident in the mAbs we isolated from HVTN 105. This may suggest overall that AIDSVAX B/E is inefficient

### Figure 6. VH1 Expansion following HIV Env Vaccination

Deep VH sequencing of peripheral blood IgG<sup>+</sup> B cells isolated D7 after final immunization was performed.

(A) Total number of lineages (top) and composition of specific VH gene usage among lineages (bottom) in individual participants (n = 22) within each treatment group (T1–T4).

(B) Compositional representation of lineages per sample, ordered by size; VH1-2 lineages denoted in red.

(C) JH usages among VH1-2 lineages and non-VH1-2 lineages.

(D) HCDR3 length among VH1-2 lineages and non-VH1-2 lineages; inset number indicates number of lineages and frequency of lineages with HCDR3 length ≥ 22 amino acids.

(E) VH mutation from germline; inset number indicates number of lineages and median percentage of nucleotide mutation.

(F) Composition of IgG subclass usage by VH1-2 (left edge of bars) and non-VH1-2 (right edge of bars) sequences. The percentage of VH1-2 sequences per sample is shown in the bar plot at top.

(G) VH mutation from germline for VH1-2 sequences from T2–T4 participants based on IgG subclass. Total number of sequences and median percentage of nucleotide mutation from germline (percentage of sequences ≥ 10% mutated from germline) are indicated.

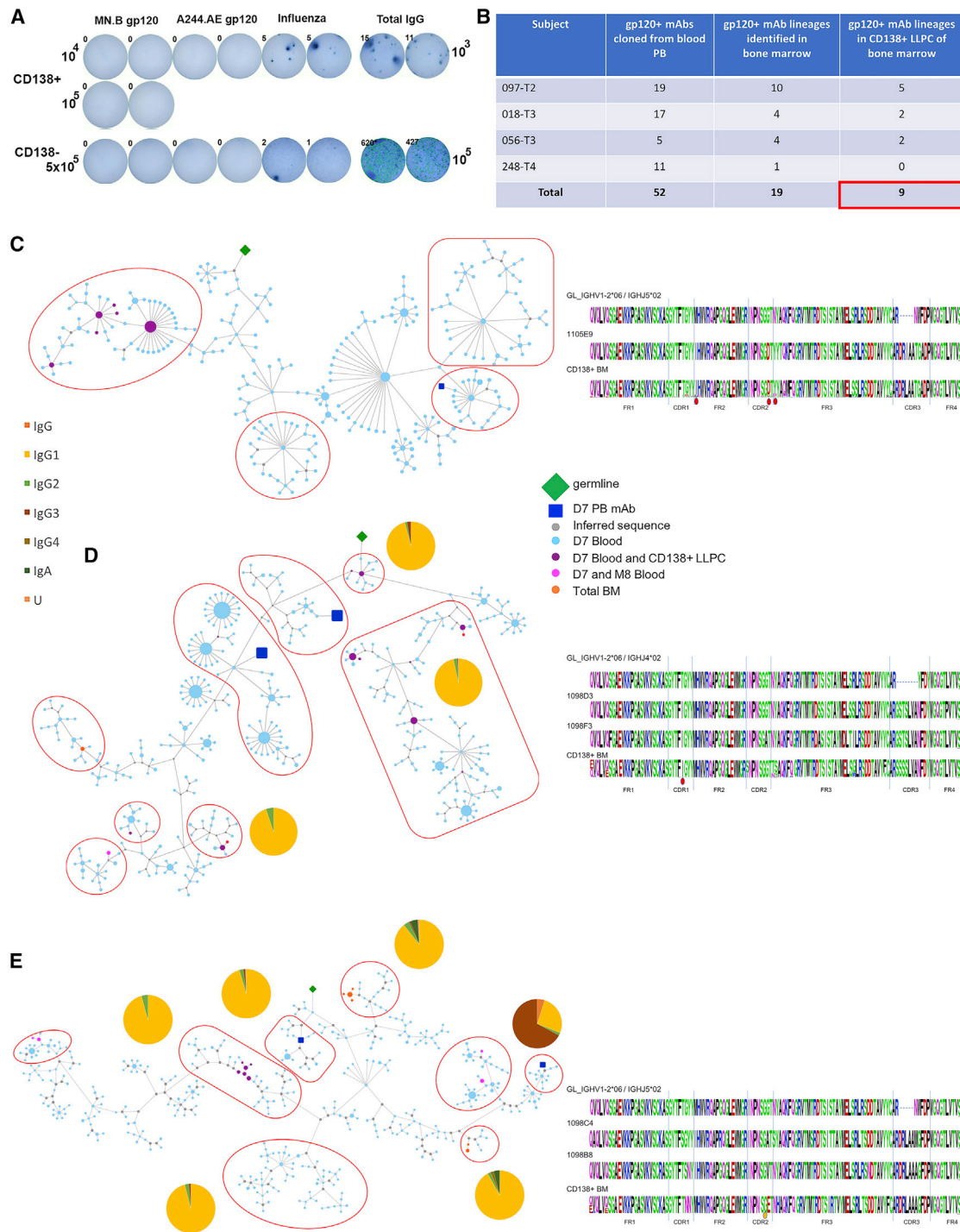


**Figure 7. Persistence of HIV Env-Specific Plasmablast Lineages in the BM LLPC**

(A) Representative Elispot of BM CD138<sup>+</sup> LLPC for gp120, influenza, and total IgG ASCs.

(B) Summary of instances of gp120<sup>+</sup> plasmablast-derived mAb lineages identified in BM. PB, plasmablast.

(C–E) Phylogenetic analysis and alignments of 1105E9 (C), 1098D3/F3 (D), and 1098C4/B8 (E) lineages. Lineage members defined as same heavy-chain V and J gene usage, HCDR3 length, and  $\geq 85\%$  HCDR3 similarity. Red-outlined regions were analyzed for isotype usage, and those for which substantial non-IgG1 sequences were observed have an associated pie chart of isotype distribution. The germline sequence is represented by the green diamond and the mAb sequences are represented by the blue square. Alignments depict germline, mAb, and CD138<sup>+</sup> LLPC derived sequences. The red circle (C and D) indicates the position of shared identical mutation from germline and the orange circle (E) indicates shared mutation from germline.

at inducing CD4bs-specific B cells and that differences in recovery in CD4bs-specific mAbs between RV305 and our study may be a consequence of the B cell subset screened (plasmablasts versus memory) or the nature of the gp120-antigen specific sorting used by Easterhoff et al.<sup>37</sup> These differences may also be a consequence of priming agent, canarypox vector (ALVAC) in RV144 versus DNA plasmid in HVTN 105, or other varying aspects between these trials.

Easterhoff et al.<sup>37</sup> isolated Env-reactive mAbs from memory B cells post-RV144 and observed that 2.1% had HCDR3s  $\geq$  22 amino acids, which is lower than the 15% observed among the mAbs in this study of HVTN 105, another AIDSVAX B/E-based regimen. Easterhoff et al. also observed that in RV305, the memory-derived Env-reactive mAbs were further skewed toward long HCDR3s antibodies ( $\sim$ 21% of the mAbs). Our deep sequencing analysis revealed that long HCDR3 are more prevalent (19%) among the VH1-2 lineages, particularly within the AIDSVAX B/E-boosted participants (T2, T3, and T4) compared to the non-VH1-2 lineages (11.7%) and compared to the VH1-2 lineages in the participants that were not boosted with AIDSVAX B/E (T1, 11.0%). The VH1-2 lineages from AIDSVAX B/E-boosted participants had a strong bias toward J6 usage, which is the longest J segment and previously reported to be overrepresented in VH1-2 antibodies with long HCDR3s, including those encoding HIV bNAbs.<sup>53,54</sup> These results suggest that HVTN 105 is more effective at promoting the development of Env-reactive B cells with longer HCDR3s than RV144. Additional boosting of HVTN 105 participants may further drive the enrichment of Env reactive with longer HCDR3s. However, the true contribution or value of Env-reactive Abs with long HCDR3s in a primarily neutralization-independent protective response such as that thought to be induced by AIDSVAX B/E remains unclear. These findings may suggest that DNA-protein regimens such as in HVTN 105 can aid in enriching for long HCDR3 utilization and should be further evaluated in trials with immunogens that promote more neutralizing Ab-dependent protection.

A dominance of VH1-2 usage by mAbs isolated following Env immunization has been noted previously.<sup>12,55</sup> Our results are consistent with this and suggest that VH1-2 dominance is not constrained to B cells targeting a specific region of Env (e.g., CD4bs), but it may be a more general phenomenon in response to particular Env protein immunizations. Although much has been resolved regarding VRC01 class Abs and their constrained usage of VH1-2 and VH1-46 and germline features that contribute to Env binding, the molecular basis of VH1-2 dominance in Env-specific non-CD4bs responses is unclear. VH1-2 usage is more pronounced among marginal zone B cells than naive B cells or switched memory B cells and increased among splenic marginal zone B cell lymphoma.<sup>56–59</sup> This adds to the speculation that some Env-specific B cell responses may develop not as a result of an initial engagement of a Env and a B cell receptor (BCR) on a naive B cell, but perhaps as engagement of BCR on a pre-existing cross-reactive memory B cell, such as marginal zone B cells, which may have initially expanded through BCR engagement with gut flora or other non-HIV antigens. The findings of Williams et al.<sup>60,61</sup> highlight the cross-reactivity of Env-specific B cells, particularly gp41 and microbial antigens. Our observed trend toward decreased somatic hyper-

mutation combined with longer HCDR3s observed among the VH1-2 mAbs and VH1-2-induced AIDSVAX B/E repertoire may suggest that the pre-existing VH1-2 repertoire, whether contained in the naive or cross-reactive memory pools, may have increased intrinsic reactivity to gp120, compared to other VH-encoded lineages. By precisely tracking the origin of Env vaccine-induced B cells, a clearer understanding of the initial B cells that respond to Env and give rise to protective responses may be obtained.

Overall, given the minimal neutralizing activity of AIDSVAX-induced Abs, Fc-dependent effector functions are thought to be a potential mechanism of protection in RV144. ADCC did not appear to be a substantial feature of these plasmablast-derived mAbs we isolated. We suspect that this may be a consequence of the initial screening process of these mAbs based on soluble Env binding, and that screening the plasmablast repertoire for ADCC activity directly is likely to identify that ADCC is a more prevalent feature than we have previously observed. This would be consistent with the majority of the HVTN 105 participants' developing ADCC plasma Abs.<sup>31</sup> ADCP is another notable Fc-dependent effector function, which in non-human primates has been correlated with vaccine-mediated protection.<sup>10,14–16</sup> Although approximately half of the mAbs demonstrated at least modest ADCP activity, only a few mediated strong ADCP activity. There was no obvious segregation of ADCP-mediating mAbs with other features such as epitope specificity or VH usage, suggesting that ADCP can be mediated by diverse Env-specific mAbs. Examination of ADCP activity using various phagocytic cells, Ab isotypes, or subclasses may reveal yet unrealized commonalities among potent ADCP-mediating mAbs.

Much attention has rightfully been given to determining whether the IgG<sub>3</sub> signal observed in RV144 associated with a decreased risk of infection is just a surrogate correlate of protection, reflecting overall variation in the quality of the humoral response compared to other AIDSVAX B/E studies, without directly mediating viral clearance, or if IgG<sub>3</sub>-mediated viral clearance such as through ADCC is truly a major direct mediator of protection. At the BCR level, IgG<sub>3</sub> was present at <10% in the AIDSVAX B/E -induced repertoire. Based on the low incidence of and lower somatic hypermutation among the IgG<sub>3</sub> repertoire, along with the increased expansion of the further mutated IgG<sub>2</sub> and IgG<sub>4</sub> in T4, it is suggested that AIDSVAX B/E-induced gp120-specific IgG<sub>3</sub>-expressing B cells are largely transitory, fading likely in part due to continued class switching to IgG<sub>1</sub>, IgG<sub>2b</sub>, IgG<sub>4</sub>, or IgA<sub>2</sub>. Thus, inducing a sustained high frequency of gp120-specific IgG<sub>3</sub>-expressing B cells may require extreme precision in the tuning of immunogen dosing and adjuvant, which may be a substantial undertaking for HIV vaccine development.

A sustained population of HIV Env Ab-producing LLPCs is expected to be a major determinant of durable vaccine-mediated protection. That Env-specific BM LLPCs were not consistently detected by EliSpot in contrast to those specific for influenza suggests that the frequency of Env-specific LLPCs is near the level of detection of the assay. Using the VH deep sequencing approach, we were able to detect the persistence of  $\sim$ 35% of the Env-specific peripheral blood plasmablast lineages in the BM, including  $\sim$ 17% that were present in LLPCs. These

Env-specific LLPCs primarily expressed IgG<sub>1</sub>; however, several instances of IgG<sub>3</sub>-expressing LLPCs among multiple lineages were apparent. These findings indicate that HIV Env immunizations in humans do induce BM LLPCs, which represent a substantial fraction of the induced peripheral blood Env-specific repertoire but comprise a relatively low frequency of the overall LLPC compartment. Efforts to more precisely quantify the frequency of HIV Env-specific lineages that make up the LLPC, relevant to other vaccine-induced responses such as influenza and measles, including the efficiency, dynamics, and regulation of seeding the LLPC compartment after repeat immunizations, are necessary to sufficiently understand and manipulate durable protective immunity to HIV.

## STAR★METHODS

Detailed methods are provided in the online version of this paper and include the following:

- **KEY RESOURCES TABLE**
- **RESOURCE AVAILABILITY**
  - Lead Contact
  - Materials Availability
  - Data and Code Availability
- **EXPERIMENTAL MODEL AND SUBJECT DETAILS**
  - Study participants / Experimental design
  - Cell Lines
- **METHOD DETAILS**
  - HIV-specific antibody secreting cells (ASC) ELISpot
  - mAb generation
  - ELISA
  - Epitope mapping
  - Antibody-Dependent Cellular Phagocytosis (ADCP) assay
  - Antibody Dependent Cellular Cytotoxicity (ADCC) Assay
  - TZM-bl neutralization assay
  - VH Next-Generational Sequencing
- **QUANTIFICATION AND STATISTICAL ANALYSIS**
- **ADDITIONAL RESOURCES**

## SUPPLEMENTAL INFORMATION

Supplemental Information can be found online at <https://doi.org/10.1016/j.xcrm.2020.100015>.

## ACKNOWLEDGMENTS

We are grateful for the assistance of the Rochester Victory Alliance and its staff. We are grateful for the technical assistance provided by Danielle DeLooze, Kevin Jin, Inho Cha, Claire Ruben, and Haien Son and for the assistance of the University of Rochester Flow Cytometry Core Facility and the University of Rochester Genomic Research Core. We are most grateful for the participation of the HVTN 105 study volunteers and thank the HVTN protocol team for their support of this project. We are very appreciative of the assistance provided by the HIV Vaccine Trials Network in enabling and coordinating this project, with particular acknowledgment of Cecilia Morgan. We are thankful to Dr. Kevin Saunders of Duke University for providing plasmid and technical advice and to Dr. Nancy Haigwood of Oregon Health & Science University-Oregon National Primate Research Center (OHSU-ONPRC) for helpful advice in preparing the manuscript. This research was partially funded by

the National Institutes of Health (NIH) (5R21AI116285, 5R01AI117787, to J.J.K.; UM1AI069511, to M.C.K.; and UM1AI068614, to C.F. as part of the HVTN Research and Mentorship Program [RAMP]), and the University of Rochester Center for AIDS Research P30AI078498 (National Institute of Allergy and Infectious Diseases [NIAID]).

## AUTHOR CONTRIBUTIONS

M.B., C.A.B., A.F.R., A.J.H., J.L.L., M.C.K., and J.J.K. conceived and designed the study. M.B., M.S.P., C.F., F.R., B.Z., and D.S. performed the experiments. M.B., C.F.F., A.F.R., and J.J.K. performed the data curation and analysis. M.B., A.F.R., and J.J.K. drafted and edited the manuscript.

## DECLARATION OF INTERESTS

The authors declare no competing interests.

Received: September 19, 2019

Revised: October 22, 2019

Accepted: April 23, 2020

Published: May 19, 2020

## REFERENCES

1. WHO (2017). HIV/AIDS Data and Statistics. <https://www.who.int/hiv/data/en>.
2. Excler, J.L., and Michael, N.L. (2016). Lessons from HIV-1 vaccine efficacy trials. *Curr. Opin. HIV AIDS* *11*, 607–613.
3. Rerks-Ngarm, S., Pitisuttithum, P., Nitayaphan, S., Kaewkungwal, J., Chiu, J., Paris, R., Premisri, N., Namwat, C., de Souza, M., Adams, E., et al.; MOPH-TAVEG Investigators (2009). Vaccination with ALVAC and AIDSVAX to prevent HIV-1 infection in Thailand. *N. Engl. J. Med.* *361*, 2209–2220.
4. Robb, M.L., Rerks-Ngarm, S., Nitayaphan, S., Pitisuttithum, P., Kaewkungwal, J., Kunasol, P., Khamboonruang, C., Thongcharoen, P., Morgan, P., Benenson, M., et al. (2012). Risk behaviour and time as covariates for efficacy of the HIV vaccine regimen ALVAC-HIV (vCP1521) and AIDSVAX B/E: a post-hoc analysis of the Thai phase 3 efficacy trial RV 144. *Lancet Infect. Dis.* *12*, 531–537.
5. Haynes, B.F., Gilbert, P.B., McElrath, M.J., Zolla-Pazner, S., Tomaras, G.D., Alam, S.M., Evans, D.T., Montefiori, D.C., Karnasuta, C., Sutthent, R., et al. (2012). Immune-correlates analysis of an HIV-1 vaccine efficacy trial. *N. Engl. J. Med.* *366*, 1275–1286.
6. Karasavvas, N., Billings, E., Rao, M., Williams, C., Zolla-Pazner, S., Bailer, R.T., Koup, R.A., Madnote, S., Arworn, D., Shen, X., et al.; MOPH TAVEG Collaboration (2012). The Thai Phase III HIV Type 1 Vaccine trial (RV144) regimen induces antibodies that target conserved regions within the V2 loop of gp120. *AIDS Res. Hum. Retroviruses* *28*, 1444–1457.
7. Zolla-Pazner, S., deCamp, A., Gilbert, P.B., Williams, C., Yates, N.L., Williams, W.T., Howington, R., Fong, Y., Morris, D.E., Soderberg, K.A., et al. (2014). Vaccine-induced IgG antibodies to V1V2 regions of multiple HIV-1 subtypes correlate with decreased risk of HIV-1 infection. *PLoS One* *9*, e87572.
8. Zolla-Pazner, S., deCamp, A.C., Cardozo, T., Karasavvas, N., Gottardo, R., Williams, C., Morris, D.E., Tomaras, G., Rao, M., Billings, E., et al. (2013). Analysis of V2 antibody responses induced in vaccinees in the ALVAC/AIDSVAX HIV-1 vaccine efficacy trial. *PLoS One* *8*, e53629.
9. Yates, N.L., Liao, H.X., Fong, Y., deCamp, A., Vandergrift, N.A., Williams, W.T., Alam, S.M., Ferrari, G., Yang, Z.Y., Seaton, K.E., et al. (2014). Vaccine-induced Env V1-V2 IgG3 correlates with lower HIV-1 infection risk and declines soon after vaccination. *Sci. Transl. Med.* *6*, 228ra39.
10. Chung, A.W., Kumar, M.P., Arnold, K.B., Yu, W.H., Schoen, M.K., Dunphy, L.J., Suscovich, T.J., Frahm, N., Linde, C., Mahan, A.E., et al. (2015). Dissecting Polyclonal Vaccine-Induced Humoral Immunity against HIV Using Systems Serology. *Cell* *163*, 988–998.

11. Tomaras, G.D., Ferrari, G., Shen, X., Alam, S.M., Liao, H.X., Pollara, J., Bonsignori, M., Moody, M.A., Fong, Y., Chen, X., et al. (2013). Vaccine-induced plasma IgA specific for the C1 region of the HIV-1 envelope blocks binding and effector function of IgG. *Proc. Natl. Acad. Sci. USA* *110*, 9019–9024.
12. Bonsignori, M., Pollara, J., Moody, M.A., Alpert, M.D., Chen, X., Hwang, K.K., Gilbert, P.B., Huang, Y., Gurley, T.C., Kozink, D.M., et al. (2012). Antibody-dependent cellular cytotoxicity-mediating antibodies from an HIV-1 vaccine efficacy trial target multiple epitopes and preferentially use the VH1 gene family. *J. Virol.* *86*, 11521–11532.
13. Chung, A.W., Ghebremichael, M., Robinson, H., Brown, E., Choi, I., Lane, S., Dugast, A.S., Schoen, M.K., Rolland, M., Suscovich, T.J., et al. (2014). Polyfunctional Fc-effector profiles mediated by IgG subclass selection distinguish RV144 and VAX003 vaccines. *Sci. Transl. Med.* *6*, 228ra38.
14. Barouch, D.H., Stephenson, K.E., Borducchi, E.N., Smith, K., Stanley, K., McNally, A.G., Liu, J., Abbink, P., Maxfield, L.F., Seaman, M.S., et al. (2013). Protective efficacy of a global HIV-1 mosaic vaccine against heterologous SHIV challenges in rhesus monkeys. *Cell* *155*, 531–539.
15. Barouch, D.H., Alter, G., Broge, T., Linde, C., Ackerman, M.E., Brown, E.P., Borducchi, E.N., Smith, K.M., Nkolola, J.P., Liu, J., et al. (2015). Protective efficacy of adenovirus/protein vaccines against SIV challenges in rhesus monkeys. *Science* *349*, 320–324.
16. Bradley, T., Pollara, J., Santra, S., Vandergrift, N., Pittala, S., Bailey-Kellogg, C., Shen, X., Parks, R., Goodman, D., Eaton, A., et al. (2017). Pentavalent HIV-1 vaccine protects against simian-human immunodeficiency virus challenge. *Nat. Commun.* *8*, 15711.
17. Wrammert, J., Smith, K., Miller, J., Langley, W.A., Kokko, K., Larsen, C., Zheng, N.Y., Mays, I., Garman, L., Helms, C., et al. (2008). Rapid cloning of high-affinity human monoclonal antibodies against influenza virus. *Nature* *453*, 667–671.
18. Halliley, J.L., Kyu, S., Kobie, J.J., Walsh, E.E., Falsey, A.R., Randall, T.D., Treanor, J., Feng, C., Sanz, I., and Lee, F.E. (2010). Peak frequencies of circulating human influenza-specific antibody secreting cells correlate with serum antibody response after immunization. *Vaccine* *28*, 3582–3587.
19. Kyu, S.Y., Kobie, J., Yang, H., Zand, M.S., Topham, D.J., Quataert, S.A., Sanz, I., and Lee, F.E. (2009). Frequencies of human influenza-specific antibody secreting cells or plasmablasts post vaccination from fresh and frozen peripheral blood mononuclear cells. *J. Immunol. Methods* *340*, 42–47.
20. Chu, V.T., and Berek, C. (2013). The establishment of the plasma cell survival niche in the bone marrow. *Immunol. Rev.* *251*, 177–188.
21. Kometani, K., and Kurosaki, T. (2015). Differentiation and maintenance of long-lived plasma cells. *Curr. Opin. Immunol.* *33*, 64–69.
22. McMillan, R., Longmire, R.L., Yelenosky, R., Lang, J.E., Heath, V., and Craddock, C.G. (1972). Immunoglobulin synthesis by human lymphoid tissues: normal bone marrow as a major site of IgG production. *J. Immunol.* *109*, 1386–1394.
23. Weisel, F.J., Zuccarino-Catania, G.V., Chikina, M., and Shlomchik, M.J. (2016). A Temporal Switch in the Germinal Center Determines Differential Output of Memory B and Plasma Cells. *Immunity* *44*, 116–130.
24. Donius, L.R., Cheng, Y., Choi, J., Sun, Z.Y., Hanson, M., Zhang, M., Gierahn, T.M., Marquez, S., Uduman, M., Kleinstein, S.H., et al. (2016). Generation of Long-Lived Bone Marrow Plasma Cells Secreting Antibodies Specific for the HIV-1 gp41 Membrane-Proximal External Region in the Absence of Polyreactivity. *J. Virol.* *90*, 8875–8890.
25. Halliley, J.L., Tipton, C.M., Liesveld, J., Rosenberg, A.F., Darce, J., Gregoret, I.V., Popova, L., Kaminiski, D., Fucile, C.F., Albizua, I., et al. (2015). Long-Lived Plasma Cells Are Contained within the CD19(-)CD38(hi)CD138(+) Subset in Human Bone Marrow. *Immunity* *43*, 132–145.
26. Amanna, I.J., Carlson, N.E., and Slifka, M.K. (2007). Duration of humoral immunity to common viral and vaccine antigens. *N. Engl. J. Med.* *357*, 1903–1915.
27. Amanna, I.J., and Slifka, M.K. (2010). Mechanisms that determine plasma cell lifespan and the duration of humoral immunity. *Immunol. Rev.* *236*, 125–138.
28. Montezuma-Rusca, J.M., Moir, S., Kardava, L., Buckner, C.M., Louie, A., Kim, L.J., Santich, B.H., Wang, W., Fankuchen, O.R., Diaz, G., et al. (2015). Bone marrow plasma cells are a primary source of serum HIV-1-specific antibodies in chronically infected individuals. *J. Immunol.* *194*, 2561–2568.
29. Huang, K.H., Bonsall, D., Katzourakis, A., Thomson, E.C., Fidler, S.J., Main, J., Muir, D., Weber, J.N., Frater, A.J., Phillips, R.E., et al. (2010). B-cell depletion reveals a role for antibodies in the control of chronic HIV-1 infection. *Nat. Commun.* *1*, 102.
30. Sundling, C., Martinez, P., Soldaro, M., Spångberg, M., Bengtsson, K.L., Stertman, L., Forsell, M.N., and Karlsson Hedestam, G.B. (2013). Immunization of macaques with soluble HIV type 1 and influenza virus envelope glycoproteins results in a similarly rapid contraction of peripheral B-cell responses after boosting. *J. Infect. Dis.* *207*, 426–431.
31. Roupheal, N.G., Morgan, C., Li, S.S., Jensen, R., Sanchez, B., Karuna, S., Swann, E., Sobieszczyk, M.E., Frank, I., Wilson, G.J., et al.; HVTN 105 Protocol Team and the NIAID HIV Vaccine Trials Network (2019). DNA priming and gp120 boosting induces HIV-specific antibodies in a randomized clinical trial. *J. Clin. Invest.* *129*, 4769–4785.
32. González-García, I., Ocaña, E., Jiménez-Gómez, G., Campos-Caro, A., and Brieva, J.A. (2006). Immunization-induced perturbation of human blood plasma cell pool: progressive maturation, IL-6 responsiveness, and high PRDI-BF1/BLIMP1 expression are critical distinctions between antigen-specific and nonspecific plasma cells. *J. Immunol.* *176*, 4042–4050.
33. Gorny, M.K., Wang, X.H., Williams, C., Volsky, B., Revesz, K., Witover, B., Burda, S., Urbanski, M., Nyambi, P., Krachmarov, C., et al. (2009). Preferential use of the VH5-51 gene segment by the human immune response to code for antibodies against the V3 domain of HIV-1. *Mol. Immunol.* *46*, 917–926.
34. Gorny, M.K., Sampson, J., Li, H., Jiang, X., Totrov, M., Wang, X.H., Williams, C., O’Neal, T., Volsky, B., Li, L., et al. (2011). Human anti-V3 HIV-1 monoclonal antibodies encoded by the VH5-51/VL lambda genes define a conserved antigenic structure. *PLoS One* *6*, e27780.
35. Zhou, T., Georgiev, I., Wu, X., Yang, Z.Y., Dai, K., Finzi, A., Kwon, Y.D., Scheid, J.F., Shi, W., Xu, L., et al. (2010). Structural basis for broad and potent neutralization of HIV-1 by antibody VRC01. *Science* *329*, 811–817.
36. West, A.P., Jr., Diskin, R., Nussenzweig, M.C., and Bjorkman, P.J. (2012). Structural basis for germ-line gene usage of a potent class of antibodies targeting the CD4-binding site of HIV-1 gp120. *Proc. Natl. Acad. Sci. USA* *109*, E2083–E2090.
37. Easterhoff, D., Moody, M.A., Fera, D., Cheng, H., Ackerman, M., Wiehe, K., Saunders, K.O., Pollara, J., Vandergrift, N., Parks, R., et al. (2017). Boosting of HIV envelope CD4 binding site antibodies with long variable heavy third complementarity determining region in the randomized double blind RV305 HIV-1 vaccine trial. *PLoS Pathog.* *13*, e1006182.
38. Walker, L.M., Phogat, S.K., Chan-Hui, P.Y., Wagner, D., Phung, P., Goss, J.L., Wrin, T., Simek, M.D., Fling, S., Mitcham, J.L., et al.; Protocol G Principal Investigators (2009). Broad and potent neutralizing antibodies from an African donor reveal a new HIV-1 vaccine target. *Science* *326*, 285–289.
39. Bonsignori, M., Hwang, K.K., Chen, X., Tsao, C.Y., Morris, L., Gray, E., Marshall, D.J., Crump, J.A., Kapiga, S.H., Sam, N.E., et al. (2011). Analysis of a clonal lineage of HIV-1 envelope V2/V3 conformational epitope-specific broadly neutralizing antibodies and their inferred unmutated common ancestors. *J. Virol.* *85*, 9998–10009.
40. Zhou, T., Lynch, R.M., Chen, L., Acharya, P., Wu, X., Doria-Rose, N.A., Joyce, M.G., Lingwood, D., Soto, C., Bailer, R.T., et al.; NISC Comparative Sequencing Program (2015). Structural Repertoire of HIV-1-Neutralizing Antibodies Targeting the CD4 Supersite in 14 Donors. *Cell* *161*, 1280–1292.
41. Walker, L.M., Huber, M., Doores, K.J., Falkowska, E., Pejchal, R., Julien, J.P., Wang, S.K., Ramos, A., Chan-Hui, P.Y., Moyle, M., et al.; Protocol

- G Principal Investigators (2011). Broad neutralization coverage of HIV by multiple highly potent antibodies. *Nature* 477, 466–470.
42. Doria-Rose, N.A., Schramm, C.A., Gorman, J., Moore, P.L., Bhiman, J.N., DeKosky, B.J., Erandes, M.J., Georgiev, I.S., Kim, H.J., Pancera, M., et al.; NISC Comparative Sequencing Program (2014). Developmental pathway for potent V1V2-directed HIV-neutralizing antibodies. *Nature* 509, 55–62.
  43. Vidarsson, G., Dekkers, G., and Rispens, T. (2014). IgG subclasses and allotypes: from structure to effector functions. *Front. Immunol.* 5, 520.
  44. Scherpenisse, M., Mollers, M., Schepp, R.M., Meijer, C.J., de Melker, H.E., Berbers, G.A., and van der Klis, F.R. (2013). Detection of systemic and mucosal HPV-specific IgG and IgA antibodies in adolescent girls one and two years after HPV vaccination. *Hum. Vaccin. Immunother.* 9, 314–321.
  45. Petäjä, T., Pedersen, C., Poder, A., Strauss, G., Catteau, G., Thomas, F., Lehtinen, M., and Descamps, D. (2011). Long-term persistence of systemic and mucosal immune response to HPV-16/18 AS04-adjuvanted vaccine in preteen/adolescent girls and young women. *Int. J. Cancer* 129, 2147–2157.
  46. Wagner, D.K., Clements, M.L., Reimer, C.B., Snyder, M., Nelson, D.L., and Murphy, B.R. (1987). Analysis of immunoglobulin G antibody responses after administration of live and inactivated influenza A vaccine indicates that nasal wash immunoglobulin G is a transudate from serum. *J. Clin. Microbiol.* 25, 559–562.
  47. Liao, H.X., Bonsignori, M., Alam, S.M., McLellan, J.S., Tomaras, G.D., Moody, M.A., Kozink, D.M., Hwang, K.K., Chen, X., Tsao, C.Y., et al. (2013). Vaccine induction of antibodies against a structurally heterogeneous site of immune pressure within HIV-1 envelope protein variable regions 1 and 2. *Immunity* 38, 176–186.
  48. Montefiori, D.C., Karnasuta, C., Huang, Y., Ahmed, H., Gilbert, P., de Souza, M.S., McLinden, R., Tovanabutra, S., Laurence-Chenine, A., Sanders-Buell, E., et al. (2012). Magnitude and breadth of the neutralizing antibody response in the RV144 and Vax003 HIV-1 vaccine efficacy trials. *J. Infect. Dis.* 206, 431–441.
  49. Balasubramanian, P., Williams, C., Shapiro, M.B., Sinangil, F., Higgins, K., Nádas, A., Totrov, M., Kong, X.P., Fiore-Gartland, A.J., Haigwood, N.L., et al. (2018). Functional Antibody Response Against V1V2 and V3 of HIV gp120 in the VAX003 and VAX004 Vaccine Trials. *Sci. Rep.* 8, 542.
  50. Jiang, X., Burke, V., Totrov, M., Williams, C., Cardozo, T., Gorny, M.K., Zolla-Pazner, S., and Kong, X.P. (2010). Conserved structural elements in the V3 crown of HIV-1 gp120. *Nat. Struct. Mol. Biol.* 17, 955–961.
  51. Gottardo, R., Bailer, R.T., Korber, B.T., Gnanakaran, S., Phillips, J., Shen, X., Tomaras, G.D., Turk, E., Imholte, G., Eckler, L., et al. (2013). Plasma IgG to linear epitopes in the V2 and V3 regions of HIV-1 gp120 correlate with a reduced risk of infection in the RV144 vaccine efficacy trial. *PLoS One* 8, e75665.
  52. Zolla-Pazner, S., Edlefsen, P.T., Rolland, M., Kong, X.P., deCamp, A., Gottardo, R., Williams, C., Tovanabutra, S., Sharpe-Cohen, S., Mullins, J.I., et al. (2014). Vaccine-induced Human Antibodies Specific for the Third Variable Region of HIV-1 gp120 Impose Immune Pressure on Infecting Viruses. *EBioMedicine* 1, 37–45.
  53. Yu, L., and Guan, Y. (2014). Immunologic Basis for Long HCDR3s in Broadly Neutralizing Antibodies Against HIV-1. *Front. Immunol.* 5, 250.
  54. Briney, B.S., Willis, J.R., and Crowe, J.E., Jr. (2012). Human peripheral blood antibodies with long HCDR3s are established primarily at original recombination using a limited subset of germline genes. *PLoS One* 7, e36750.
  55. Costa, M.R., Pollara, J., Edwards, R.W., Seaman, M.S., Gorny, M.K., Montefiori, D.C., Liao, H.X., Ferrari, G., Lu, S., and Wang, S. (2016). Fc Receptor-Mediated Activities of Env-Specific Human Monoclonal Antibodies Generated from Volunteers Receiving the DNA Prime-Protein Boost HIV Vaccine DP6-001. *J. Virol.* 90, 10362–10378.
  56. Michaeli, M., Tabibian-Keissar, H., Schiby, G., Shahaf, G., Pickman, Y., Hazanov, L., Rosenblatt, K., Dunn-Walters, D.K., Barshack, I., and Mehr, R. (2014). Immunoglobulin gene repertoire diversification and selection in the stomach - from gastritis to gastric lymphomas. *Front. Immunol.* 5, 264.
  57. Julakyan, U.L., Biderman, B.V., Gemdzian, E.G., Sudarikov, A.B., and Savchenko, V.G. (2015). [Molecular analysis of immunoglobulin genes in the tumor B cells in splenic marginal zone lymphoma]. *Ter. Arkh.* 87, 58–63.
  58. Bikos, V., Darzentas, N., Hadzidimitriou, A., Davis, Z., Hockley, S., Traverse-Glehen, A., Algara, P., Santoro, A., Gonzalez, D., Mollejo, M., et al. (2012). Over 30% of patients with splenic marginal zone lymphoma express the same immunoglobulin heavy variable gene: ontogenetic implications. *Leukemia* 26, 1638–1646.
  59. Pujanauski, L.M., Janoff, E.N., McCarter, M.D., Pelanda, R., and Torres, R.M. (2013). Mouse marginal zone B cells harbor specificities similar to human broadly neutralizing HIV antibodies. *Proc. Natl. Acad. Sci. USA* 110, 1422–1427.
  60. Williams, W.B., Han, Q., and Haynes, B.F. (2018). Cross-reactivity of HIV vaccine responses and the microbiome. *Curr. Opin. HIV AIDS* 13, 9–14.
  61. Williams, W.B., Liao, H.X., Moody, M.A., Kepler, T.B., Alam, S.M., Gao, F., Wiehe, K., Trama, A.M., Jones, K., Zhang, R., et al. (2015). HIV-1 VACCINES. Diversion of HIV-1 vaccine-induced immunity by gp41-microbiota cross-reactive antibodies. *Science* 349, aab1253.
  62. Howell, D.N., Andreotti, P.E., Dawson, J.R., and Cresswell, P. (1985). Natural killing target antigens as inducers of interferon: studies with an immunoselected, natural killing-resistant human T lymphoblastoid cell line. *J. Immunol.* 134, 971–976.
  63. Trkola, A., Matthews, J., Gordon, C., Ketas, T., and Moore, J.P. (1999). A cell line-based neutralization assay for primary human immunodeficiency virus type 1 isolates that use either the CCR5 or the CXCR4 coreceptor. *J. Virol.* 73, 8966–8974.
  64. Yagita, M., Huang, C.L., Umehara, H., Matsuo, Y., Tabata, R., Miyake, M., Konaka, Y., and Takatsuki, K. (2000). A novel natural killer cell line (KHYG-1) from a patient with aggressive natural killer cell leukemia carrying a p53 point mutation. *Leukemia* 14, 922–930.
  65. Kobie, J.J., Alcena, D.C., Zheng, B., Bryk, P., Mattiaccio, J.L., Brewer, M., Labranche, C., Young, F.M., Dewhurst, S., Montefiori, D.C., et al. (2012). 9G4 autoreactivity is increased in HIV-infected patients and correlates with HIV broadly neutralizing serum activity. *PLoS One* 7, e35356.
  66. Kobie, J.J., Zheng, B., Bryk, P., Barnes, M., Ritchlin, C.T., Tabechian, D.A., Anandarajah, A.P., Looney, R.J., Thiele, R.G., Anolik, J.H., et al. (2011). Decreased influenza-specific B cell responses in rheumatoid arthritis patients treated with anti-tumor necrosis factor. *Arthritis Res. Ther.* 13, R209.
  67. Nogales, A., Piepenbrink, M.S., Wang, J., Ortega, S., Basu, M., Fucile, C.F., Treanor, J.J., Rosenberg, A.F., Zand, M.S., Keefer, M.C., et al. (2018). A Highly Potent and Broadly Neutralizing H1 Influenza-Specific Human Monoclonal Antibody. *Sci. Rep.* 8, 4374.
  68. Liao, H.X., Levesque, M.C., Nagel, A., Dixon, A., Zhang, R., Walter, E., Parks, R., Whitesides, J., Marshall, D.J., Hwang, K.K., et al. (2009). High-throughput isolation of immunoglobulin genes from single human B cells and expression as monoclonal antibodies. *J. Virol. Methods* 158, 171–179.
  69. Tiller, T., Meffre, E., Yurasov, S., Tsuiji, M., Nussenzweig, M.C., and Wardemann, H. (2008). Efficient generation of monoclonal antibodies from single human B cells by single cell RT-PCR and expression vector cloning. *J. Immunol. Methods* 329, 112–124.
  70. Kobie, J.J., Zheng, B., Piepenbrink, M.S., Hessell, A.J., Haigwood, N.L., Keefer, M.C., and Sanz, I. (2015). Functional and Molecular Characteristics of Novel and Conserved Cross-Clade HIV Envelope Specific Human Monoclonal Antibodies. *Monoclon. Antib. Immunodiagn. Immunother.* 34, 65–72.

71. Ackerman, M.E., Moldt, B., Wyatt, R.T., Dugast, A.S., McAndrew, E., Tsoukas, S., Jost, S., Berger, C.T., Sciaranghella, G., Liu, Q., et al. (2011). A robust, high-throughput assay to determine the phagocytic activity of clinical antibody samples. *J. Immunol. Methods* **366**, 8–19.
72. Alpert, M.D., Heyer, L.N., Williams, D.E., Harvey, J.D., Greenough, T., Allhorn, M., and Evans, D.T. (2012). A novel assay for antibody-dependent cell-mediated cytotoxicity against HIV-1- or SIV-infected cells reveals incomplete overlap with antibodies measured by neutralization and binding assays. *J. Virol.* **86**, 12039–12052.
73. Blay, W.M., Kasprzyk, T., Misher, L., Richardson, B.A., and Haigwood, N.L. (2007). Mutations in envelope gp120 can impact proteolytic processing of the gp160 precursor and thereby affect neutralization sensitivity of human immunodeficiency virus type 1 pseudoviruses. *J. Virol.* **81**, 13037–13049.
74. Wei, X., Decker, J.M., Wang, S., Hui, H., Kappes, J.C., Wu, X., Salazar-Gonzalez, J.F., Salazar, M.G., Kilby, J.M., Saag, M.S., et al. (2003). Antibody neutralization and escape by HIV-1. *Nature* **422**, 307–312.
75. Montefiori, D.C. (2009). Measuring HIV neutralization in a luciferase reporter gene assay. *Methods Mol. Biol.* **485**, 395–405.
76. Khan, S., Nakajima, R., Jain, A., de Assis, R.R., Jasinskas, A., Obiero, J.M., Adenaiye, O., Tai, S., Hong, F., Milton, D.K., et al. (2020). Analysis of Serologic Cross-Reactivity Between Common Human Coronaviruses and SARS-CoV-2 Using Coronavirus Antigen Microarray. *bioRxiv*. <https://doi.org/10.1101/2020.03.24.006544>.
77. Piepenbrink, M.S., Nogales, A., Basu, M., Fucile, F.F., Liesveld, J.L., Keefer, M.C., Rosenberg, A.F., Martinez-Sobrido, L., and Kobie, J.J. (2019). Broad and Protective Influenza B Virus Neuraminidase Antibodies in Humans after Vaccination and their Clonal Persistence as Plasma Cells. *mBio*, Published online March 12, 2019. <https://doi.org/10.1128/mBio.00066-19>.
78. Tipton, C.M., Fucile, C.F., Darce, J., Chida, A., Ichikawa, T., Gregoret, I., Schieferl, S., Hom, J., Jenks, S., Feldman, R.J., et al. (2015). Diversity, cellular origin and autoreactivity of antibody-secreting cell population expansions in acute systemic lupus erythematosus. *Nat. Immunol.* **16**, 755–765.
79. Aouinti, S., Giudicelli, V., Duroux, P., Malouche, D., Kossida, S., and Lefranc, M.P. (2016). IMGT/StatClonotype for Pairwise Evaluation and Visualization of NGS IG and TR IMGT Clonotype (AA) Diversity or Expression from IMGT/HighV-QUEST. *Front. Immunol.* **7**, 339.
80. Felsenstein, J. (2005). PHYLIP (Phylogeny Inference Package) version 3.6 (Department of Genome Sciences, University of Washington).
81. Shannon, P., Markiel, A., Ozier, O., Baliga, N.S., Wang, J.T., Ramage, D., Amin, N., Schwikowski, B., and Ideker, T. (2003). Cytoscape: a software environment for integrated models of biomolecular interaction networks. *Genome Res.* **13**, 2498–2504.

STAR★METHODS

KEY RESOURCES TABLE

REAGENT or RESOURCE	SOURCE	IDENTIFIER
<b>Antibodies</b>		
anti-CD45-Qdot 800 (HI30)	Thermo Fisher Scientific	Cat#Q10156; RRID:AB_10373711
APC-Cy7 Mouse Anti-Human CD19 (SJ25C1)	BD Biosciences	Cat#557791; RRID:AB_396873
Alexa Fluor® 700 anti-human CD20 (2H7)	Biolegend	Cat#302322; RRID:AB_493753
anti-CD3e-PacificOrange (UCHT1)	Invitrogen	Cat#CD0330; RRID:AB_2536469
FITC Mouse Anti-Human IgD (IA6-2)	BD Biosciences	Cat#555778; RRID:AB_396113
anti-CD27-Qdot 655 (CLB-27/1)	Thermo Fisher Scientific	Cat#Q10066; RRID:AB_11180873
anti-CD4-Qdot 705 (S3.5)	Thermo Fisher Scientific	Cat#Q10060; RRID:AB_2556447
anti-CD38-Qdot 605 (HIT2)	Thermo Fisher Scientific	Cat#Q10053; RRID:AB_2556444
anti-CD126-PE (M5)	BD Biosciences	Cat#561696; RRID:AB_10896139
Goat Anti-Human IgG Antibody (Peroxidase)	Jackson ImmunoResearch	Cat#109-035-003; RRID:AB_2337577
alkaline phosphatase-conjugated anti-human IgG	Jackson ImmunoResearch	Cat#109-055-003; RRID:AB_2337599
AffiniPure F(ab') <sub>2</sub> Fragment Goat Anti-Human IgG, F(ab') <sub>2</sub> fragment specific	Jackson ImmunoResearch	Cat#109-006-097
<b>Bacterial and Virus Strains</b>		
DH5a	Thermo Fisher Scientific	Cat#18265017
SHIV SF162P3 Virus	NIH AIDS Reagent Program	Cat#6526
<b>Biological Samples</b>		
Human blood from HVTN105 study participants	URMC CFAR	N/A
Human bone marrow from HVTN105 study participants	URMC CFAR	N/A
<b>Chemicals, Peptides, and Recombinant Proteins</b>		
MN.B D11 gp120	NIH AIDS Reagent Program	Cat#12570
A244.AE D11 gp120	NIH AIDS Reagent Program	Cat#12569
FluZone (2006-2007)	Sanofi Pasteur	Cat# NR-10483
96ZM651 gp120	NIH AIDS Reagent Program	Cat#10080
A244_V1V2 tag	NIH AIDS Reagent Program	Cat#12567
C1086_V1V2	NIH AIDS Reagent Program	Cat#12568
Resurfaced stabilized core (RSC3) protein	NIH AIDS Reagent Program	Cat#12042
HIV-1 Subtype B (MN) Env Peptide Set	NIH AIDS Reagent Program	Cat#6451
HIV-1 Consensus Group M Env Peptide Set	NIH AIDS Reagent Program	Cat#9487
HIV-1 Consensus B V3 Peptide	NIH AIDS Reagent Program	Cat#1830
HIV-1 Subtype B (Sequence 1) V3 Peptide	NIH AIDS Reagent Program	Cat#1831
HIV-1 MN V3 Peptide	NIH AIDS Reagent Program	Cat#1832
HIV-1 RF V3 Peptide	NIH AIDS Reagent Program	Cat#1833
HIV-1 SF2 V3 Peptide	NIH AIDS Reagent Program	Cat#1834
HIV-1 CRF01_AE V3 Peptide	NIH AIDS Reagent Program	Cat#1835
HIV-1 Subtype B (Sequence 2) V3 Peptide	NIH AIDS Reagent Program	Cat#1836
HIV-1 Consensus B V3 Cyclic Peptide	NIH AIDS Reagent Program	Cat#1837
HIV-1 Subtype B (Sequence 2) V3 Cyclic Peptide	NIH AIDS Reagent Program	Cat#1839

(Continued on next page)



**Continued**

REAGENT or RESOURCE	SOURCE	IDENTIFIER
HIV-1 MN Complete V3 Loop Peptide	NIH AIDS Reagent Program	Cat#1840
Phosphate Buffered Saline (PBS)	Corning	Cat#21-040-CV
RPMI1640	Corning	Cat#15-040-CV
Fetal Bovine Serum (FBS)	Atlanta Biologicals	Cat#S12450H
Tween 20	Biorad	Cat#1706531
2-Mercaptoethanol	Millipore Sigma	Cat# M3148
VECTOR Blue, Alkaline Phosphatase Substrate Kit III	Vector Laboratories	Cat#SK-5300
DTT	Invitrogen	Cat#P2325
RiboLock RNase Inhibitor	ThermoFisher	Cat#EO0381
qScript cDNA synthesis kit	QuantaBio	Cat#95047-100
DMEM	GIBCO	Cat#10313039
FetalClone II	GE Healthcare Life Sciences	Cat#SH30066.03
Antibiotic-Antimycotic solution	GIBCO	Cat#15240062
jetPRIME transfection reagent	PolyPlus	Cat#114-75
Magna Protein G beads	Promega	Cat#G7472
Magna Protein A beads	Promega	Cat#G8782
Bovine Serum Albumin (BSA)	Fischer Scientific	Cat#BP1600100
Trypsin-EDTA	ThermoFisher	Cat#25300054
Biotin-XX Microscale Protein Labeling Kit	Life Technologies	Cat#B30010
Yellow-Green streptavidin- fluorescent beads	Life Technologies	Cat#F8776
Bright-Glo	Promega	Cat#E2620
RNeasy Mini Kit	QIAGEN	Cat#74104
Turbo DNA-free Kit	Invitrogen	Cat#AM1907
Platinum Taq High Fidelity Polymerase	Invitrogen	Cat#11304011
EconoTaq PLUS GREEN 2X Master Mix	Lucigen	Cat# 30033-2
iProof High-Fidelity DNA Polymerase	Biorad	Cat# 1725302
HotStarTaq Plus DNA Polymerase	QIAGEN	Cat# 203607
E.Z.N.A. Gel Extraction Kit	Omega Bio-tek	Cat#D2501-02
E.Z.N.A. Cycle Pure Kit	Omega Bio-tek	Cat#D6493-02
E.Z.N.A. Plasmid Mini Kit I	Omega Bio-tek	Cat# D6942-02
Amicon® Ultra-15 Centrifugal Filter Unit	Millipore Sigma	Cat# UFC910024
<b>Critical Commercial Assays</b>		
Illumina MiSeq Reagent Kit v3	Illumina Inc.	Cat#MS-102-3003
<b>Experimental Models: Cell Lines</b>		
Human THP-1 cells	NIH AIDS Reagent Program	Cat#9942; RRID:CVCL_0006
CEM.NKR CCR5+Luc+ (NKR24)	NIH AIDS Reagent Program	Cat#5198; RRID:CVCL_X624
KHG1 rhCD16	Japan Health Sciences Foundation	N/A
HeLA-derived TZM-bl cells	NIH AIDS Reagent Program	Cat#8129; RRID:CVCL_B478
HEK293T	ATCC	Cat#CRL-3216; RRID:CVCL_0063
<b>Oligonucleotides</b>		
Primers for mAb generation	Liao et al., 2009	PMID:19428587
Primers for MiSeq <a href="#">Table 1</a>	This paper	N/A
<b>Software and Algorithms</b>		
CTL immunospot	Cellular Technology Limited	<a href="http://www.immunospot.com/ImmunoSpot-analyzers-software">http://www.immunospot.com/ImmunoSpot-analyzers-software</a>
IMGT/V-QUEST		<a href="http://www.imgt.org/IMGT_vquest/vquest">http://www.imgt.org/IMGT_vquest/vquest</a>

(Continued on next page)

<b>Continued</b>		
REAGENT or RESOURCE	SOURCE	IDENTIFIER
GraphPad Prism v7.0	<a href="https://www.graphpad.com/scientific-software/prism/">https://www.graphpad.com/scientific-software/prism/</a>	N/A
Flowjo	<a href="https://www.flowjo.com/">https://www.flowjo.com/</a>	N/A
HighV-QUEST		<a href="https://www.imgt.org/HighV-QUEST/home.action">https://www.imgt.org/HighV-QUEST/home.action</a>
Phylip's protpars tool (version 3.695)	<a href="http://evolution.genetics.washington.edu/phylip.html">http://evolution.genetics.washington.edu/phylip.html</a>	N/A
Cytoscape	<a href="https://cytoscape.org/">https://cytoscape.org/</a>	N/A
MATLAB	MathWorks	<a href="https://www.mathworks.com/products/matlab.html">https://www.mathworks.com/products/matlab.html</a>
Deposited Data		
Antibody and repertoire RNA sequences	dbGaP	dbGaP:phs002027.v1.p1

## RESOURCE AVAILABILITY

### Lead Contact

Further information and requests for resources should be directed to the Lead Contact, James Kobie ([jjkobie@uabmc.edu](mailto:jjkobie@uabmc.edu)).

### Materials Availability

All unique/stable reagents generated in this study are available from the Lead Contact with a completed Materials Transfer Agreement.

### Data and Code Availability

The antibody and repertoire RNA sequences are available from the database of Genotypes and Phenotypes (dbGaP) (<https://www.ncbi.nlm.nih.gov/gap/>) accession accession phs002027.v1.p1.

## EXPERIMENTAL MODEL AND SUBJECT DETAILS

### Study participants / Experimental design

Blood and tissue samples for this study were obtained from 22 participants at the University of Rochester who participated in the HVTN 105 phase 1 randomized, blinded, multisite HIV vaccine clinical trial ([ClinicalTrials.gov](https://clinicaltrials.gov/ct2/show/study/NCT02207920) NCT02207920).<sup>31</sup> Sample size estimation was not applicable to this study as sample size was determined by the number of participants from the clinical trial at the University of Rochester site who agreed to provide these additional samples. Participants were assigned to experimental groups by the clinical trial. All procedures used in this study were approved by the Research Subjects Review Board at the University of Rochester Medical Center and all participants provided written informed consent. All participants were seronegative for HIV infection at the time of enrollment for the study. Participants received different combinations of AIDSVAX® B/E (HIV envelope gp120 of clade B (MN) and E (A244)), DNA-HIV-PT123 (3 plasmids containing DNA of clade C ZM96 gag, clade C ZM96 gp140 and clade C CN54 pol-nef) and placebo administered intra-muscularly at 4 time points over a period of 6 months (Figure 1). Peripheral blood mononuclear cells (PBMCs) and plasma were obtained prior to the vaccination, 7 days post final vaccination and ~7 months post final vaccination. Bone marrow aspirate was obtained ~7 months post final vaccination.

### Cell Lines

HEK293T cells (ATCC) were used for transient transfection to produce recombinant human monoclonal antibodies. The cells were cultured at 37°C with 5% CO<sub>2</sub> saturation in DMEM (GIBCO, Life Technologies) supplemented with 10% FetalClone II (GE Healthcare Life Sciences) and 1x antibiotic/antimycotic solution (GIBCO, Life Technologies).

THP-1 cells (NIH AIDS Reagent Program) were cultured in RPMI1640 (Corning) medium supplemented with 2-mercaptoethanol (Millipore sigma) to a final concentration of 0.05 mM and 10% fetal bovine serum (Atlanta Biologicals). Cultures were maintained by the addition or replacement of fresh medium every 2 to 3 days to maintain the cell concentration ~5x10<sup>5</sup> cells/ml (below 1 × 10<sup>6</sup> cells/ml).

NKR24 luciferase-reporter cell line were derived from CEM.NKR.CCR5 CD4+ T cells<sup>62,63</sup> and obtained from the AIDS Research and Reference Reagent Program.

KHYG-1 rhCD16 effector cells were derived from the CD16-negative human NK cell line KHYG-1 (Japan Health Sciences Foundation).<sup>64</sup>

TZM-bl cells are used for HIV-1 pseudovirus neutralization assays and are obtained from the NIHARRP. Complete growth medium (GM) consists of D-MEM supplemented with 10% fetal bovine serum (FBS, heat-inactivated), 25 mM HEPES and 50  $\mu\text{g}/\text{ml}$  gentamicin. TZM-bl is an adherent cell line that can be disrupted and removed by treatment with trypsin/EDTA at confluency for routine maintenance and for assay preparation. Cultures should be passaged up to a maximum of 20 times every 2-3 days with approximately  $10^6$  cells in 15ml of GM. Cultures are incubated at 37°C in a 5% CO<sub>2</sub>/95% air environment.

## METHOD DETAILS

### HIV-specific antibody secreting cells (ASC) ELISpot

The frequency of HIV-specific ASC in total PBMC were determined by ELISpot similar to as previously described.<sup>65,66</sup> Briefly, sterile 96-well PVDF membrane plates (MilliporeSigma, USA) were coated overnight at 4°C with 50  $\mu\text{L}$  of 5  $\mu\text{g}/\text{ml}$  HIV1 Env MN.B D11 gp120 or A244.AE D11 gp120 (NIH AIDS Reagent Program), 6  $\mu\text{g}/\text{ml}$  FluZone (2006-2007) or 1  $\mu\text{g}/\text{ml}$  anti-human IgG (Jackson ImmunoResearch, West Grove, PA) in PBS. Plates were blocked with RPMI1640 (Corning, VA, USA) media with 10% fetal bovine serum (Atlanta Biologicals, GA, USA) for 2 h at 37°C. Then 100,000 and 500,000 PBMCs (for Ag specific wells) or 10,000 and 20,000 PBMCs (for total IgG-specific wells) in a final volume of 200  $\mu\text{L}$  were added per well in triplicate. The plates were incubated for ~40 hours at 37°C in 5% CO<sub>2</sub> and then washed with PBS containing 0.1% Tween 20. Bound antibodies were detected with 50  $\mu\text{L}$  of 1  $\mu\text{g}/\text{ml}$  alkaline phosphatase-conjugated anti-human IgG (diluted in PBS containing 0.1% Tween 20 and 1% BSA) antibody (Jackson ImmunoResearch, West Grove, PA) for 2 hours at 37°C in 5% CO<sub>2</sub> and then developed with VECTOR Blue, Alkaline Phosphatase Substrate Kit III (Vector Laboratories, Burlingame, CA). The spots per well were counted using the CTL immunospot reader (Cellular Technologies Ltd., Shaker Heights, OH, USA).

### mAb generation

For monoclonal antibody (mAb) generation, plasmablasts were single cell sorted from PBMCs isolated 7 days post final vaccination as previously described by Nogales et al.<sup>67</sup> with a FACSAria cell sorter (BD Biosciences) directly into 96-well PCR plates (Bio-Rad, Hercules, CA) containing 4  $\mu\text{L}/\text{well}$  0.5X PBS with 10 mM DTT (Invitrogen), and 8 U RiboLock (ThermoFisher) RNase inhibitor. Immunoglobulin heavy, kappa and lambda variable regions were amplified with two rounds of semiquantitative RT-PCR. Primers used for these PCRs were described in Liao et al.<sup>68</sup> Purified PCR products were sequenced at Genewiz (<https://www.genewiz.com/en>) or ACGT (<https://www.acgtinc.com/>) and sequencing results were analyzed by IMGTV-QUEST ([www.imgt.org/IMGTV\\_quest](http://www.imgt.org/IMGTV_quest)) to determine germline V(D)J gene segments with highest identity. These PCR-amplified V-regions were then used to construct linear heavy and light chain Ig cassettes as previously described<sup>68</sup> for transient expressions in a 96 well plate format which allows quick and efficient handling of large number of samples. Approximately 25,000 human embryonic kidney (HEK293T; ATCC) cells/well were seeded in a 96 well plate with 100  $\mu\text{L}$  of DMEM (GIBCO, Life Technologies, NY, USA) containing 10% FetalClone II (GE Healthcare Life Sciences, UT, USA) and 1x antibiotic/antimycotic solution (GIBCO, Life Technologies, NY) and incubated at 37°C with 5% CO<sub>2</sub> for ~24-36 hours. 70%–80% confluent cells were transfected with the purified linear cassettes using jetPRIME® transfection reagent (PolyPlus, NY, USA) and incubated at 37°C with 5% CO<sub>2</sub> for 5 days. Cell culture supernatants were collected and screened for HIV Env gp120 (MN.B and A244.AE) reactivity by enzyme-linked immunosorbent assay (ELISA). Clones that showed positive result in screening ELISA were selected for large scale production. Expression of recombinant mAbs as full human IgG1 was performed as described previously.<sup>69,70</sup> After 8 days of transfection mAbs were purified from culture supernatant using Magna Protein G or A beads (Promega, WI, USA).

### ELISA

The reactivity profiles of plasma IgG and isolated mAbs against HIV Env proteins were detected by ELISA. Briefly, ELISA plates (Nunc MaxiSorp; Thermo Fisher Scientific, NY, USA) were coated overnight at 4°C with 50  $\mu\text{L}$  of 0.5  $\mu\text{g}/\text{ml}$  HIV Env gp120 (MN.B, A244.AE or 96ZM651.C, NIH AIDS Reagent Program) in PBS and blocked with 3% BSA in PBS for 30 min at room temperature. Plasma samples were tested at 1:2500 dilution and mAbs were tested at 10-fold dilutions (10, 1 and 0.1  $\mu\text{g}/\text{ml}$ ). 50  $\mu\text{L}$  of the samples (diluted in PBS containing 0.05% Tween 20 or PBST) were added per well in triplicate and incubated for 1 h. The reaction was detected using peroxidase-conjugated anti-human IgG (Jackson ImmunoResearch, PA, USA), diluted 1:2000 in PBST. mAbs that showed OD<sub>450</sub>  $\geq$  1 @ 10  $\mu\text{g}/\text{ml}$  against MN.B or A244.AE were defined as gp120+ and included in this study. Mean OD values of triplicate test samples were divided by control (PBST) and represented as relative units (RU). Overall binding strength (avidity) of the selected mAbs at 10  $\mu\text{g}/\text{ml}$  was evaluated in presence of 8M urea for 15 min at room temperature prior to the addition of detection antibody. Avidity Index calculated as OD<sub>450</sub> in presence of urea / OD<sub>450</sub> in absence of urea.

### Epitope mapping

Detection of V1V2 and CD4-binding site specific mAbs were performed following previously described ELISA protocol against A244\_V1V2 tag, C1086\_V1V2 or RSC3 (NIH AIDS Reagent Program). Epitope specificity of isolated mAbs (1  $\mu\text{g}/\text{ml}$ ) were performed using overlapping 15-mer linear peptides (5  $\mu\text{g}/\text{ml}$ ) spanning the gp160 Env (MN.B or M.Cons strains, NIH AIDS Reagent Program). V3 region specific reactivity of the isolated mAbs were further confirmed using HIV Env V3 cyclic peptide and complete V3 loop peptide (NIH AIDS Reagent Program).

### Antibody-Dependent Cellular Phagocytosis (ADCP) assay

ADCP activity of the mAbs was measured as previously described<sup>71</sup> with slight modifications. Briefly, HIV Env gp120 (MN.B and A244.AE) were biotinylated with the Biotin-XX Microscale Protein Labeling Kit (Life Technologies, NY, USA). 0.25  $\mu\text{g}$  of biotinylated Ag or 0.14  $\mu\text{g}$  of BSA (used as a baseline control in an equivalent number of Ag molecules / bead) was incubated overnight at 4°C with  $1.8 \times 10^6$  Yellow-Green streptavidin- fluorescent beads (Life Technologies) per reaction in a 25  $\mu\text{L}$  of final volume. Antigen-coated beads were subsequently washed twice in PBS-BSA (0.1%) and transferred to a 5 mL Falcon round bottom tube (Thermo Fisher Scientific, NY, USA). mAbs, diluted at 5  $\mu\text{g}/\text{mL}$ , were added to each tube in a 20  $\mu\text{L}$  of reaction volume and incubated for a 2 h at 37°C in order to allow Ag-Ab binding. Then 250,000 THP-1 cells (human monocytic cell line obtained from NIH AIDS Reagent Program) were added to the cells and incubated for 3 h at 37°C. At the end of incubation, 100  $\mu\text{L}$  4% paraformaldehyde was added to fix the samples. Cells were then assayed for fluorescent bead uptake by flow cytometry using a BD Biosciences LSR II. The phagocytic score of each sample was calculated by multiplying the percentage of bead positive cells (frequency) by the degree of phagocytosis measured as mean fluorescence intensity (MFI) and dividing by  $10^6$ . Values were normalized to background values (cells and beads without mAb) and an isotype control to ensure consistency in values obtained on different assays. Finally, the phagocytic score of the testing mAb was expressed as the fold increase over BSA-coated beads.

### Antibody Dependent Cellular Cytotoxicity (ADCC) Assay

Determination of mAb ADCC activity was performed as previously described.<sup>72</sup> In brief,  $\text{CD4}^+\text{CCR5}^+$  NKR24 target cells that express luciferase under control of a tat-dependent promoter were infected with replication competent SHIV<sub>SF162p3</sub> (200 ng/ml p27) by spinoculation at 1200 x g for 2 hr in the presence of 40  $\mu\text{g}/\text{mL}$  polybrene. Once infection was established (3 DPI),  $1 \times 10^4$  target cells/well were co-incubated with KHYG-1  $\text{Fc}\gamma\text{RIIIa}$  (CD16)<sup>+</sup> NK effector cells at an effector to target ratio of 10:1 with or without serial mAb dilutions in 200  $\mu\text{L}$  assay media (RPMI supplemented with 5 U/ml IL-2) in round bottom 96 well plates at 37°C and 5%  $\text{CO}_2$ . All mAb dilutions were plated in duplicate. After 8 hr co-incubation, wells were thoroughly mixed by pipetting, and 150  $\mu\text{L}$  cells transferred to wells in black flat bottom plates containing 50  $\mu\text{L}$  Bright-Glo (Promega) and incubated for 2 min at 25°C. Luminescence was measured on a Victor X Light plate reader (Perkin Elmer) and relative light units (RLU) were normalized according to the following formula:  $[\text{sample mean} - \text{background} (\text{mock-infected targets and effectors})] / [\text{maximum} (\text{SHIV-infected targets and effectors, no mAb} - \text{background})] \times 100$ . ADCC activity is reported as the percentage loss of RLU.

### TZM-bl neutralization assay

mAbs were tested for their ability to neutralize HIV-1 Env-containing pseudoviruses using the single-cycle TZM-bl neutralization assay as described previously.<sup>73–75</sup> As a negative control, a mAb against an irrelevant antigen was included (not shown). Neutralization dose-response curves were fitted by nonlinear regression and a final titer is reported as the reciprocal of the dilution of serum necessary to achieve 50% neutralization. For mAbs the concentration of Ab required to obtain 50% neutralization (the  $\text{IC}_{50}$ ) is reported.

### VH Next-Generational Sequencing

For the Ig VH sequencing library preparation, PBMCs and plasmablasts were collected 7 days post final vaccination and bone marrow (CD138+ fraction, CD138- fraction or total) and peripheral blood B cells were collected ~7 months post final vaccination. Total RNA was isolated using the RNeasy Mini Kit (QIAGEN, Germany) and treated with DNase I (Turbo DNA-free Kit, Invitrogen, Lithuania). Approximately 1/10 part of this RNA was used for cDNA synthesis in a 20  $\mu\text{L}$  reaction with the qScript cDNA synthesis kit (QuantaBio, MA, USA). A PCR was carried out in a 50  $\mu\text{L}$  reaction using Platinum Taq High Fidelity Polymerase (Invitrogen, Carlsbad, CA) with 5  $\mu\text{L}$  of the resulting cDNA as template. A cocktail of degenerate VH1, VH2, VH3, VH4, VH5 and VH6 (0.5  $\mu\text{M}$  each) forward primers from framework region (FR)1 and a cocktail of isotypes (IgA, IgG and/or IgM) specific (2  $\mu\text{M}$  each) reverse primer from constant domain 1. For targeted VH gene specific libraries, forward primers were designed from either Ig leader or FR1 regions (Table S1). Each forward and reverse primer contained a 12 nucleotide index and the Illumina specific linker (forward: CAAGCAGAAG ACGGCATACGAGATGTGACTGGAGTTCAGACGTGTGCTCTTCCGATCT, reverse: AATGATACGGCGACCACCGAGATCTACACTC TTTCCTACACGAGCTCTTCCGATCT) sequence. The 45 cycles touch-down PCR condition was as follows: one cycle of initial denaturation at 95°C for 5 min followed by 2 cycles of 95°C for 30 s, 65°C for 30 s, 68°C for 1 min; after every 2 cycles the annealing temperature was dropped 2°C for four times; then 35 cycles of 95°C for 30 s, 57°C for 30 s, 68°C for 1 min and a final extension at 72°C for 10 min.

Following PCR, amplicons were analyzed in 1% agarose gel and bands corresponding to approximately 600 bp was purified with E.Z.N.A.™ Gel Extraction Kit (Omega Bio-tek, GA, USA). Purified products were submitted to the University of Rochester Genomics Research Center, where quality control was performed using Qubit fluorometer (Thermo Fisher) and Bioanalyzer (Agilent Technologies, Santa Clara, CA). Finally, the PCR products were pooled together in equimolar ratio and sequenced on an Illumina MiSeq system (Illumina, Inc., CA, USA) using 300 x 325 bp paired-end kits (Illumina MiSeq Reagent Kit v3, 600-cycle, Illumina Inc., CA, USA). Sequence analysis was performed using an in-house custom analysis pipeline described previously.<sup>67,76–78</sup> Briefly, all sequences were aligned with [www.imgt.org/HighV-QUEST](http://www.imgt.org/HighV-QUEST)<sup>79</sup> following quality filtering and paired-read joining. Sequences were then analyzed for V region mutations and clonality. All clonal lineage assignments were based on identical VH and JH regions, identical HCDR3 length and > 85% HCDR3 nucleotide homology. Lineage trees were generated for lineages containing mAb sequences (by including

the mAbs in the clonal lineage assignment step). Sequences within a lineage with single occurrences of particular VDJ amino acid sequences (singletons) were removed, with the exception of singletons that match any inferred node sequence. The resulting sequences were analyzed using Phylip's protpars tool (version 3.69 s), turning on settings 1, 4, and 5.<sup>80</sup> The output file was then parsed using in-house custom scripts, collapsing any duplicate sequences into an individual node, and was visualized using Cytoscape.<sup>81</sup>

**Table 1. Primers Used in This Study**

Primer	Sequences (5' -3')
VH1-Fw	CAGGTGCAGCTGGTRCARTCTGGG
VH2-Fw	CAGRGCACCTTGARGGAGTCTGGTCC
VH3-Fw	GAGGTKCAGCTGGTGGAGTCTGGG
VH4-Fw	ACCCTGTCCCTCACCTGC
VH5-Fw	GCAGCTGGTGCAGTCTGGAG
VH6-Fw	CAGGACTGGTGAAGCCCTCG
VH1-24/69-Fw	GCAGCAGCTACAGGTGCCASKCC
VH1-2-Fw	GCAGCAGCCACAGGAGCCCACTCC
VH3-23-Fw	AGTTTGGGCTGAGCTGGCTT
VH3-23(M13)-Fw	TTCTCAGGTGCAGCTGGTGC
IgA-Rv	GAGGCTCAGCGGAAGACCTTG
IgG-Rv	GGAAGGTGTGCACGCCGCTGGTC
IgM-Rv	GTGATGGAGTCGGGAAGGAA

## QUANTIFICATION AND STATISTICAL ANALYSIS

Statistical analysis of VH deep sequencing data was done with Graphpad Prism v7.0 or MATLAB, using unpaired Mann-Whitney test or Wilcoxon matched-pairs signed rank test as appropriate. Statistical details of experiments can be found in the figures and figure legends. Spearman correlation was used to determine how effective the pairing was.

## ADDITIONAL RESOURCES

Samples used for this study were obtained from at the University of Rochester who participated in the HVTN 105 phase 1 randomized, blinded, multisite HIV vaccine clinical trial ([ClinicalTrials.gov](https://clinicaltrials.gov/ct2/show/study/NCT02207920) NCT02207920)<sup>31</sup>.